SPECTROSCOPIC CHARACTERIZATION OF BILIARY TRACT TISSUES IN-VIVO TO ASSIST LAPAROSCOPIC CHOLECYSTECTOMY

by

SARITA KOMMERA

Presented to the Faculty of the Graduate School of

The University of Texas at Arlington in Partial Fulfillment

of the Requirements

for the Degree of

MASTER OF SCIENCE IN BIOMEDICAL ENGINEERING

THE UNIVERSITY OF TEXAS AT ARLINGTON

December 2006

ACKNOWLEDGEMENTS

I would to thank many people who made this thesis possible. I want to express my gratitude to my supervising professor, Dr. Hanli Liu, who had been a major inspiration to me. Her enthusiasm to explain all the things clearly has made this thesis a very good learning experience to me in the field of Bio-engineering. I would also like to thank Dr. Livingston for his ultimate support and the knowledge he imparted to me about laparoscopic surgery and the problems faced by the surgeons which have made my work interesting. I am indebted to Dr. Wang for all the wise advices provided by him. I am also thankful to Ronnie Brown and Dr. Park for proving us with a subject and helping me take all the readings and without their help it would have been a very difficult to get a very appealing outcome from the thesis. I would also like to thank Dr. Rose for his help in performing surgery on the pigs.

I am grateful to all my lab mates, Dheerendra Kashyap and Praveen Gulaka in particular for being a huge support regardless of the matter.

Lastly, and more importantly, I would like to thank my elder brothers and my parents, Satyanarayana Kommera and Vijaya Lakshmi Kommera for their immense support. They have raised me, educated me and supported me in all the aspects. I am thankful to my husband, Kiran , for all the emotional support and help. I would like to dedicate my thesis to my father whom I love the most.

November 1, 2006

ABSTRACT

SPECTROSCOPIC CHARACTERIZATION OF BILIARY TRACT TISSUES IN-VIVO TO ASSIST LAPAROSCOPIC CHOLECYSTECTOMY

Publication No. _____

Sarita Kommera, MS

The University of Texas at Arlington, 2006

Supervising Professor: Dr. Hanli Liu

Laparoscopic Cholecystectomy is a surgical method for removal of gallbladder when it is diseased with gall stones. Almost 750,000 people are affected with this disease annually in USA. Gall bladder is removed by placing an incision on the cystic duct. This duct is totally embedded in fat (which is a few mm thick) in most of the cases and it becomes a huge problem decreasing the visual capability of the surgeon to distinctly locate the duct.

Near Infrared Spectroscopy (NIRS) can solve the fuzziness as it penetrates in a few mm thick tissues. NIRS is one of the techniques used for studying the physiological properties of the biological tissue. Light delivered into the tissue undergoes multiple scattering and absorption, and reflects back carrying quantitative

information. Light attenuation in the Near Infrared Red (700-900nm) region is relatively less by tissue chromophores thus allowing to study their variation in this wavelength region.

This study was initiated by the clinical problem mentioned above, and it aimed to investigate the spectroscopic characterization of biliary tract tissues measured in vivo using animal models. The goal of the study is to develop an intraoperative imaging tool to be used for guiding laparoscopic cholecystectomy. Specifically, 8 living pigs were used for the in vivo experiments, The animal biliary tract tissues, including gall, common bile duct (CBD), and cystic duct, were measured using a CCD-array spectrometer and a hand-held fiber-optic probe. The respective spectroscopic features were obtained and analyzed using the Radial Basis Function approach. Three derived parameters were developed and can be used to differentiate different types of biliary tract tissues.

TABLE OF CONTENTS

LIST OF ILLUSTRATIONS

LIST OF TABLES

CHAPTER I

INTRODUCTION

1.1. Gall Bladder

The Gallbladder is a pear-shaped organ and lies on top of the liver in the right-upper abdomen. Its major function is to store bile. It is attached to the bile ducts that come from the liver through Cystic duct. These ducts carry bile from the liver to the gallbladder and intestine where the bile helps digest food. The gallbladder is not necessary to maintain good health. The gall bladder and the ducts that carry bile and other digestive enzymes from the liver constitute the biliary system as shown in Fig 1.1.

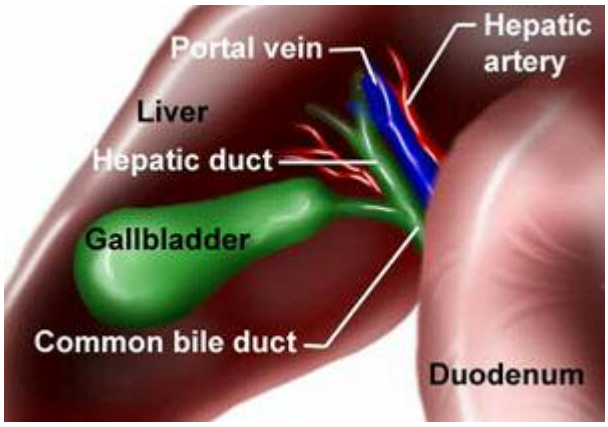

Figure 1.1 Anatomy of Biliary tract tissues

Bile is used to help the body digest fats by contracting the gall bladder which pushes the bile into the common bile duct. Bile from the common bile duct is then carried to the small intestine for digestion. Bile's major constituents are water,

cholesterol, fats, bile salts, proteins, and bilirubin. Bile salts break up fat, and bilirubin gives bile and stool a yellowish color.

1.1.1 Gall Stones

Gallstones usually form in the gallbladder due to excessive cholesterol in bile. They are a very common medical problem. Bile which is stored in the gallbladder hardens into pieces and forms stone-like material as shown in figure 1.2. If bile contains too much cholesterol, bile salts, or bilirubin, under certain conditions it can harden into stones. 80 percent of the gall stones are formed due to this reason. Gallbladder can develop just one large stone, hundreds of tiny stones, or almost any combination.

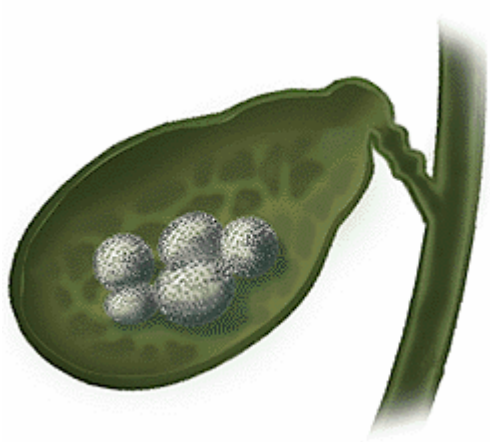

Figure 1.2 Gall Bladder with Gall Stones

Contraction of the gallbladder with stones in it will cause pain and other problems. For the treatment, the removal of the gallbladder is one of the most common types of surgery done. In the past, open abdominal surgery was the standard treatment.

This procedure required a 3 to 7 day stay in the hospital and a 3 to 7 inch incision and scar on the abdomen. Now the use of laparoscopy has been expanded to include removing a diseased gallbladder.

1.1.2 Laparoscopic Cholecystectomy

A cholecystectomy is the procedure for surgical removal of the gallbladder. Laparoscopic technology, is now used to remove the gallbladder through a tiny incision at the navel. Abdomen is inflated with carbon dioxide, a harmless gas, for a clear view and to provide room for the surgery to be performed. Two needle-like instruments are inserted which serve as tiny hands within the abdomen. They are used to pick up the gallbladder, move intestines around, and generally assist the surgeon. Finally, several different instruments are inserted to clip the gallbladder artery and bile duct, and to safely dissect and remove the gallbladder and stones. The entire procedure normally takes 30 to 60 minutes. The three puncture wounds doesn't require any stitches and may leave very slight blemishes.

1.1.3 Advantages

The main benefit of this procedure is the ease of recovery for the patient. There is no incision pan as occurs with standard abdominal surgery. In fact, up to 90% of patients are discharged the same day. And within several days, normal activities can be resumed. So the recovery time is much quicker. Also, there is no scar on the abdomen.

1.1.4 Complications

The procedure seems very easy for the patient, but, as it is still abdominal surgery, there are some complications included. It still carries the risks of the general

surgery, though infrequent.. Current medical reports indicate that the low complication rate is about the same for this procedure as for standard gallbladder surgery. These complications may include bile duct injury because of the difficulty in locating the duct. In some cases gallbladder cannot be safely removed by laparoscopy due to the fat, a few millimeters thick, lying on top of the biliary tree. Due to this fat, it becomes a huge problem for the surgeons to exactly locate the duct as there are chances to cut the hepatic artery and portal vein which runs close to the biliary ducts. Also, there is not a specified shape of the cystic duct and it is observed to be different in different persons as shown in figure 1.3.

The imaging technique that is adopted for this surgery till now is intraoperative cholangiography (IOC). This method is quite expensive. A catheter is placed into the cystic duct and a contrast is injected. An X-ray image is then obtained of the contrast-filled bile duct . The image is called intraoperative cholangiogram. This procedure has to be done frequently during gall bladder surgery to detect the common bile duct and other abnormalities. As this method is quite expensive the whole surgery would cost the patient a lot more.

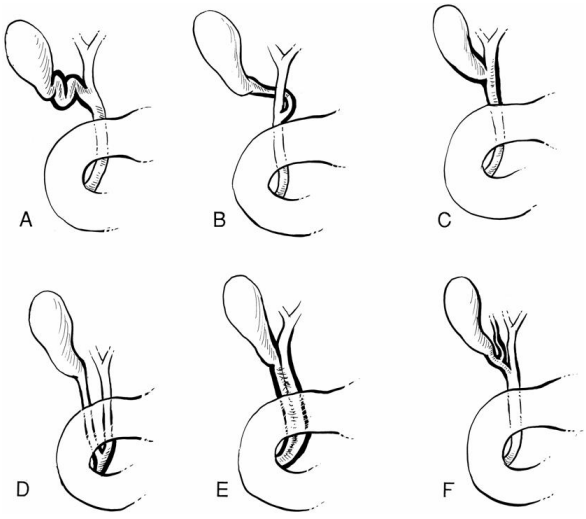

Figure 1.3 A, B, C, D, E, F show different shapes of the common bile duct and cystic duct.

In such cases, it becomes highly impossible for the surgeons to exactly locate the cystic duct and then make an incision. Common bile duct injuries can happen, and standard open abdominal surgery is then immediately performed in. Nausea and vomiting may occur after the surgery.

1.2. Near Infrared Spectroscopy

Near infrared imaging and spectroscopy is an imaging modality which monitors the changes in the states of the biological tissues using the light which is within the range of 600 to 900 nm. The light propagation in the tissues is dependent on the absorption and scattering phenomenon.

The optical properties are tissue-specific and thus enables us to study the unique optical features of different tissues. Near Infrared Spectroscopy (NIRS) measures the reflectance, due to the multiple absorption and scatterings of the chromophores, which gives us the information of the tissue quantitatively. The

absorption in the NIR region is mainly due to the presence of water, oxygenated and de-oxygenated hemoglobin which have a distinct optical spectra in the visible and the NIR region as shown in Figure 1.4. These distinct optical features in the NIR region are especially attractive for tissue imaging.

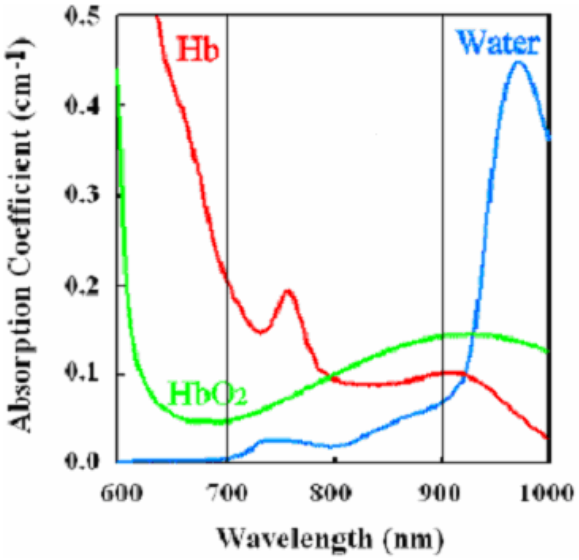

Figure 1.4 Absorption spectrum in the NIR window

The aim of this project is to develop a methodology that will allow a differentiation in optical signatures between the biliary tissues and the blood vessels which run near these ducts. This developed methodology thus enables the surgeons to have a careful demarcation between the ducts and the blood vessels. Biliary organs contains bile in them , which has a different spectral feature than the other adjacent tissues. As the ducts are embedded within fat, which is a few millimeters thick, NIR Spectroscopy is a good candidate for this development. NIR goes deep a few millimeters , so the organs lying within fat can be imaged with the help of the NIRS.

CHAPTER II

METHODS AND MATERIALS

2.1 Instrumentation used for Animal Measurements

Eight live pigs and four dead pigs were used for the study. All the live pigs were acclimatized and were placed in the same environmental conditions prior to the measurements. Measurements were taken with NIRS equipment, which included an optical fiber, a spectrometer , a tungsten halogen light source and a USB to interface the computer with the spectrometer.

2.1.1 The NIRS System

A multi-channel, broadband, NIRS system consists of a large source-detector separation probe with a single source fiber and three detector fibers. The three detector fibers have been designed such that they have different source-detector separation (0.95 cm, 1.58 cm and 2.2 cm). The schematic diagram of the probe is as shown is Figure 2.1.

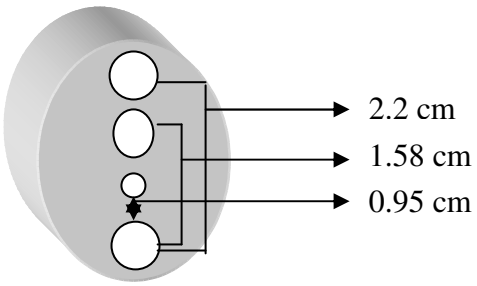

Figure 2.1. Large Separation Probe.

The three detectors also vary in diameter. The detector with a smallest source detector separation has a diameter of 0.08 cm and it is followed by detectors of diameter 0.17 cm and 0.25 cm. The measurements were taken from the abdominal tissues of the pig. Light from a tungsten-halogen lamp with continuous wave (HL2000, Ocean Optics Inc, FL) broadband light was delivered through the source fiber onto the tissue. The reflectance from the tissue was captured by the three detector fibers and passed through a multi-channel CCD array spectrometer (USB 2000 Ocean Optics, FL), as shown in Figure 2.2. The spectrometer, with the help of the USB interface, exhibits the reflectance on a laptop computer. The continuous wave system provides a spectrum from 450 nm to 900 nm from the abdominal tissues of the pig.

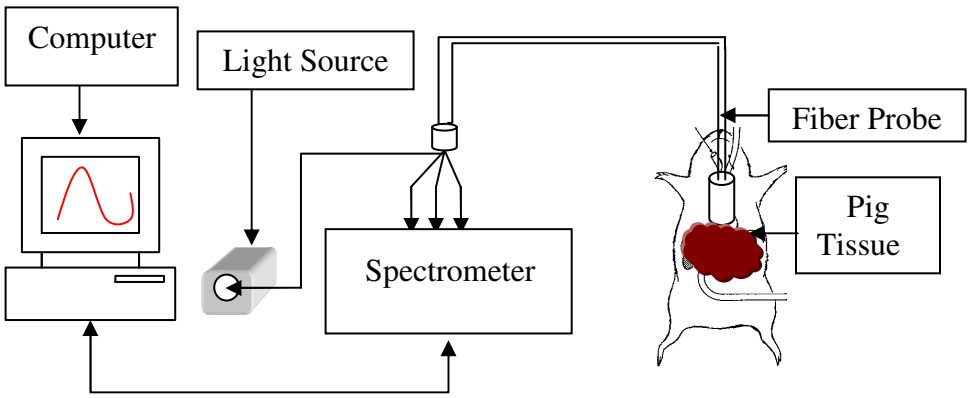

Figure 2.2. Schematic diagram of the instrumentation used.

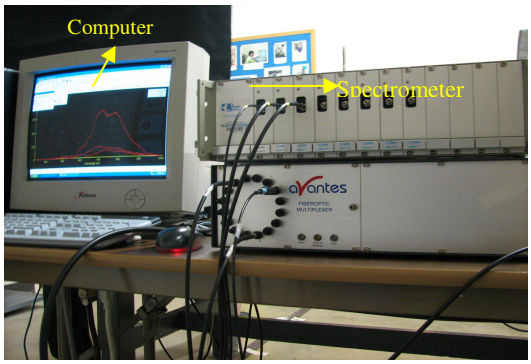

(a)

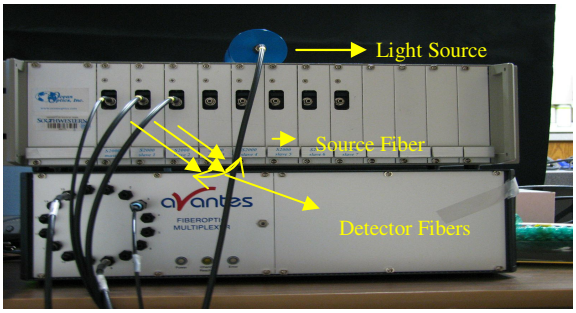

(b)

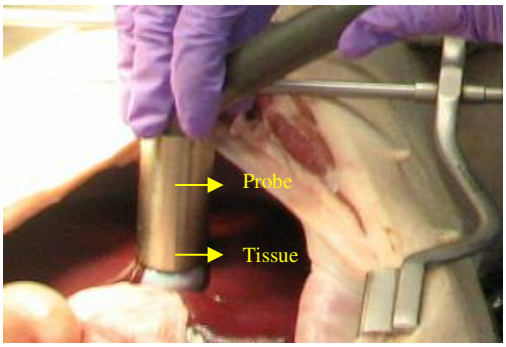

(c)

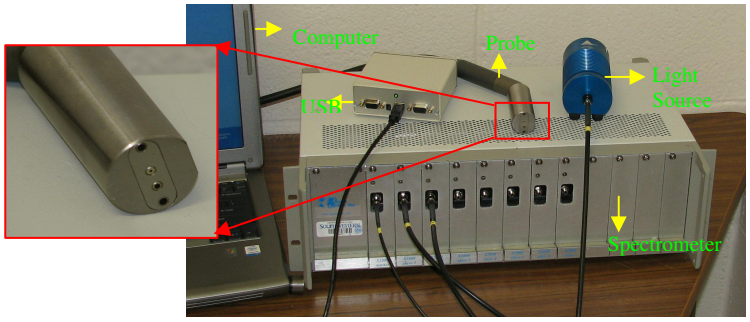

(d)

Figure 2.3 (a), (b) ,(c) and (d) represent the experimental set up.

The optical properties of the biliary tract tissues are thus studied with the spectra obtained with the large separation fiber as shown in Figure 2.3. A laptop is used for data acquisition and processing.

2.1.2 Animal Preparation

The pigs are placed in a flank position as shown in figure 2.4. The pigs are fasted for 12-16 hours before the sugery. They are anesthetized with general anesthesia. A continous supply of isofluorine and oxygen is given through the mask of the pig throughout the surgery. To maintain respiration, an endotracheal tube is inserted and is connected to the ventilator. The abdomen is prepared and draped.. An incision on the abdomen is made by the surgeon as shown in figure 2.4, and the abdomen of the pig is exposed. The multi-channel fiber optic probe is used to measure the reflectance on the biliary tract tissues, hepatic artery, and portal vein. The probe is placed on top of the tissues such that it has minimum contact with the organs. For every organ, multiple sets of measurements are collected by moving the probe on different locations. The probe is connected to the multi-channel spectrometer through which the computer records the collected data.

Figure 2.4 Animal Preparation.

2.2 Radial Basis Function

The results obtained from the reflectance measurements show unique spectral features. Radial-basis function is used as a method to differentiate the spectra for biliary tract tissues..

2.2.1 Theory

Radial basis functions (RBF) are the natural generalization of coarse coding to continuous-valued features. These functions represent various degrees to which a feature is present in the interval [0,1] , rather being 0 or 1.. A typical RBF feature i, as represented in the equation below, has a Gaussian (bell-shaped) response, Φ(i), dependent only on the distance between the state" s", and the feature's prototypical or center state" c_i ", and relative to the feature's width σ_i .

$$\phi_s(i) = \exp\left(\frac{-(s-c_i)^2}{2\sigma_i^2}\right) \qquad (2.1)$$

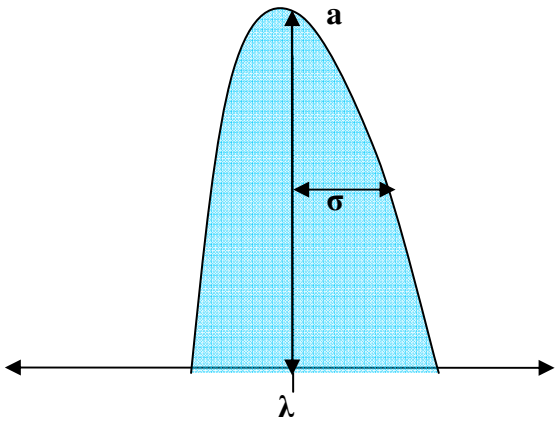

Figure 2.5 One-dimensional Radial Basis Function.

The primary advantage of Radial Basis Function over binary features is that they produce approximate functions that vary smoothly and are differentiable. In addition, some fitting methods for Radial Basis Function can be used to determine the centers and widths of the features as well. Such fitting methods may be able to fit the target function much precisely. The disadvantage of RBF fitting is the computational complexity and manual tuning.

2.2.2 Spectrum Components

After carefully observing all the spectra from different biliary tract tissues of eight live pigs, it is observed that three Gaussian waves would fit any given spectrum. As the three Gaussian waves would require three radial basis functions, equation (2.1) becomes equation (2.2)

$$S(x) = \sum_{i=1}^{N=3} a_i . e^{\left(\frac{-(\lambda - \lambda_i)^2}{2\sigma_i^2} \right)} \qquad (2.2)$$

In the above equation, 'a(i)' represents the amplitude of the Gaussian wave, 'λ(i)' represents the center wavelength and 'σ(i)' represents the width of the Gaussian wave.

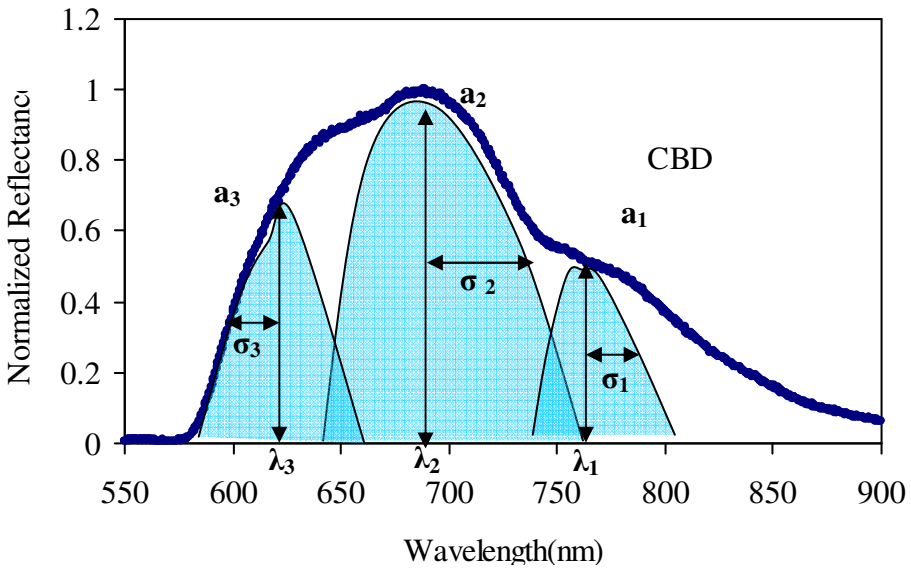

Figure 2.6 Graph representing the fit provided by the three Gaussian waves.

There are three parameters to represent a Gaussian, and the fitting requires three Gaussian's, so in total the procedure requires nine parameters as shown in Figure 2.6. From these nine parameters a classification procedure can be developed to ease the complexity.

2.3 Classification Methods

Classification methods are used to specify how different an organ is from another in terms of variables. One of the classification method used by Dr. Wang for this study is the minimum distance method. Fuzzy logic can also be employed, but it would require large amounts of data to test . A simple classification is done for this study by using only five of the nine parameters. The classification of data is divided into two categories, namely, specified classification and unspecified classification. In specified classification, classification is done with the use of true data in the form of

sample sets. In unspecified classification, classification is done with only spectral features and without using the true data.

2.3.1 Minimum distance method

Minimum distance method measures distance of the data point from each cluster. The measuring of the distance is specific to the application. The measure of several statistical distances such as Euclidean, Mahalanobis, and Bhattacharya distance are used to determine the class.

To perform a minimum distance classification, a statistical object is created with statistics for a set of regions of interest that represent training areas. The data is first classified into clusters with the truth values as shown in Figure 2.7. If the unknown point is 'x' and let m_1, c $m_2 \ldots . m_k$ be the classified clusters. The distance between the classified clusters and the unknown input is calculated as (x- m_k).

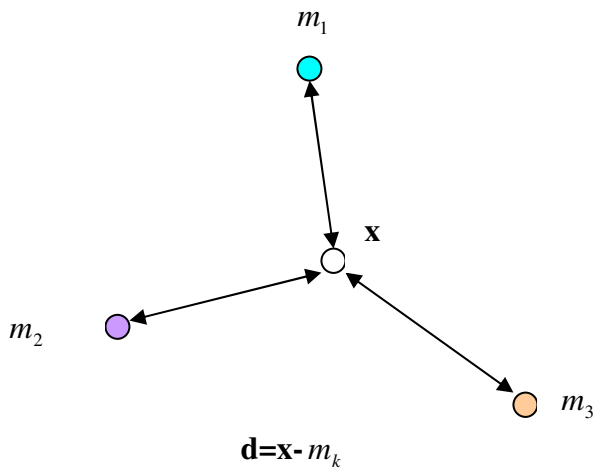

Figure 2.7 Calculation of distance from the classified clusters

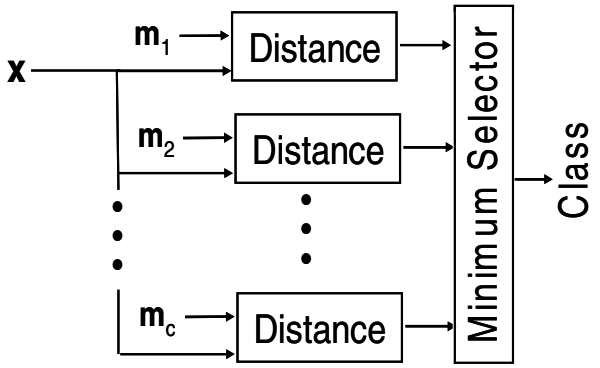

Figure 2.8 Block diagram representing the selection of minimum distance

Figure 2.8 represents iterative process in which the minimum distance is selected. In Mahalanobis, minimum distance is calculated as shown below in equation 2.3 considering the variability within the specified class and then standardizing it with respect to the new scale.

$$d(x,m)^2 = \frac{(x-m_1)^2}{v_1} + \frac{(x-m_2)^2}{v_2} + 2\frac{(x-m_1)(x-m_2)}{c_{12}} \qquad (2.3)$$

where v_1 and v_2 are the variances of the cluster m_1 and m_2 respectively. The advantages of this method are that it puts things on equal footing after transformation. Each information class has the same variation in clusters. It is closely related to probability when a normal distribution of reflectance is obeyed. Thus, one can interpret minimum distance as maximum probability or likelihood of being in a class. The disadvantage with this method is that it is too time consuming.

The data, obtained from the live pig measurements, is classified with the minimum distance method, and Mahalanobis is used to calculate the distance. The clusters are normalized to a single scale by dividing the respective distances with their

corresponding variances. Then, the data are classified into artery, biliary and vein clusters, and each cluster has a different variance.

CHAPTER III

RESULTS AND DISCUSSION

3.1 In vivo Data

Twelve pigs were measured in total. Measurements were taken on the Common Bile Duct, Cystic Duct, Gall, Hepatic Artery and Portal Vein for all the twelve pigs. Among the twelve pigs, in vivo data were collected from eight live pigs and from four dead pigs. Other abdominal tissues were also measured in some cases.

3.1.1 Pig-1 Measurements

Measurements were divided into two categories. All the measurements were taken from the first fiber, which has a source detector separation of 0.95 cm.

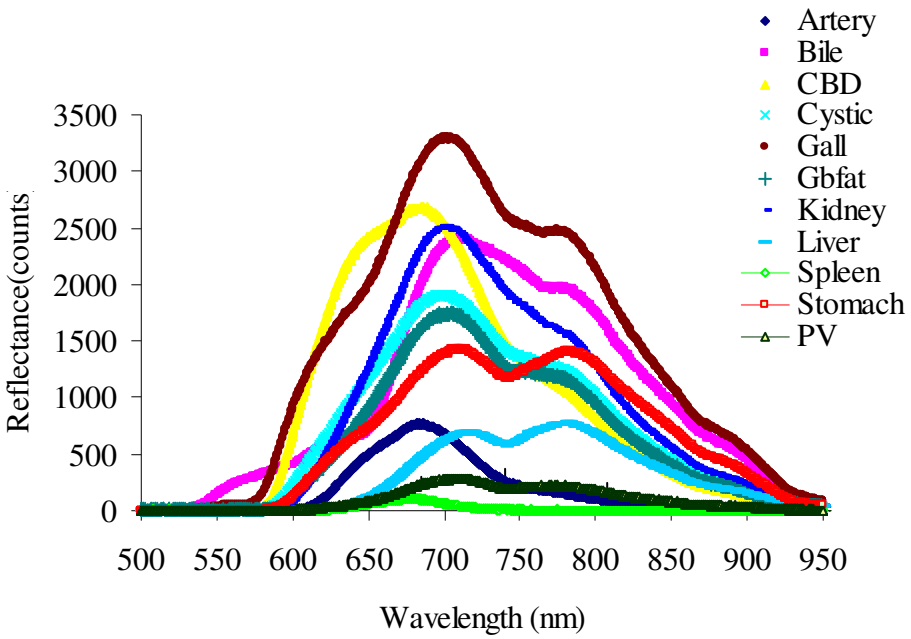

Figure 3.1 Reflectance Measurements taken on Pig-1

Abdominal tissues include liver, spleen, stomach, fat on the skin and Kidney. The project concentrates mainly on the biliary tract tissues as we are trying to find out a way to differentiate between the tissues in the biliary organs. Figure 3.1 represents the reflectance spectra from all the organs that are mentioned above. It can be shown from figure 3.1 that all the spectra are visually different with respect to shape and amplitude. Later, all the measurements are normalized to one before comparing them to one another. Biliary tract tissues and the blood vessels (Artery and Vein) have different features, and it is hypothesized that biliary tract tissues and the blood vessels have different reflectance spectra. To prove the hypothesis, the experiments were conducted on eight pigs and the data will be presented in the later sections.

3.1.2 The Five Important Organs

Laparoscopic cholecystectomy is performed to remove the gallbladder by making an incision at the cystic duct, which is connected to the right and left hepatic duct through a common bile duct. The difficulty that the surgeons face during the surgery is the immense fuzziness offered by the fat lying on the common bile duct.

This fat makes the surgeons blind to the organs lying underneath the fat. The organs that lie underneath fat can also be the hepatic artery and the portal vein, which run close to the common bile duct. Any incision to these blood vessels can be a life-threatening problem and would require additional surgeries to fix it. In some cases, the damage is irreparable and the patient can die. The five important organs in this study therefore, whose optical spectra are shown in Figure 3.2, are Common bile duct, Gall, Cystic duct, Artery and Vein.

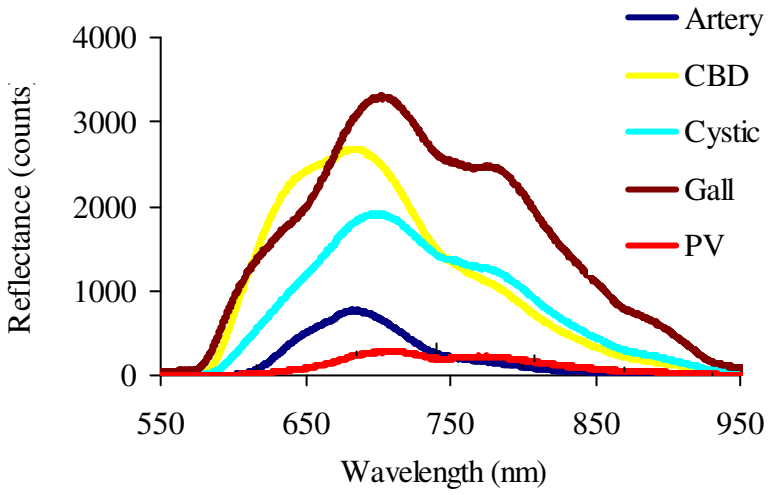

Figure 3.2 The five interested spectra

These five organs are divided into the biliary tissues and blood vessels. It is clearly shown from figure 3.2 that the five spectra that we are interested in show different reflectance profiles.

3.1.2.1 Biliary Tract Tissues

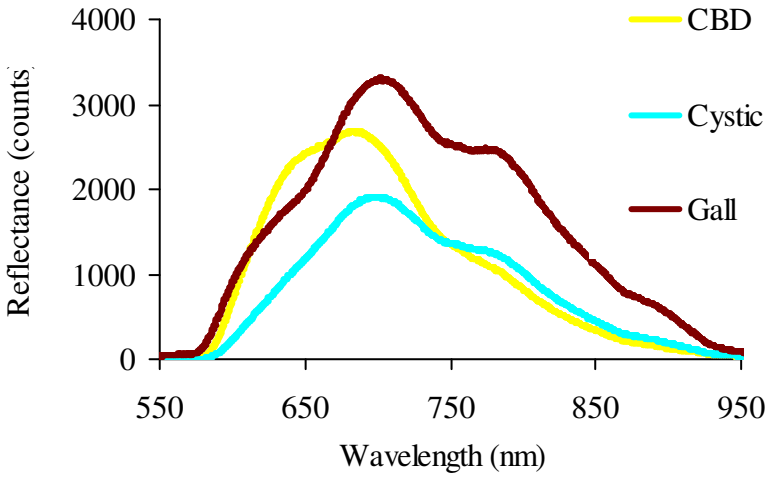

Figure 3.3 Biliary Tract Tissues

The major component of all the biliary tract tissues is bile. The chemical nature of the bile in all the pigs is not the same and so as in human beings. It is expected that there would be a resemblance between the common bile duct, gall and cystic duct as these tissue types are similar, and the major component within them is the same. However, from figure 3.3 it is observed that there is a difference among the biliary tract tissues. It might be due to the light absorption and scattering of the various lipids in the tissue, so their spectra are found different.

3.1.2.2 Blood Vessels

The Blood vessels that we are interested in are the hepatic artery and the portal vein. Figure 3.4 shows us the reflectance profiles of these two blood vessels. As an artery has oxy-hemoglobin, which is a good absorber, therefore, the magnitude of the reflectance profile is lower than the other biliary tract tissues as shown in Figure 3.2.

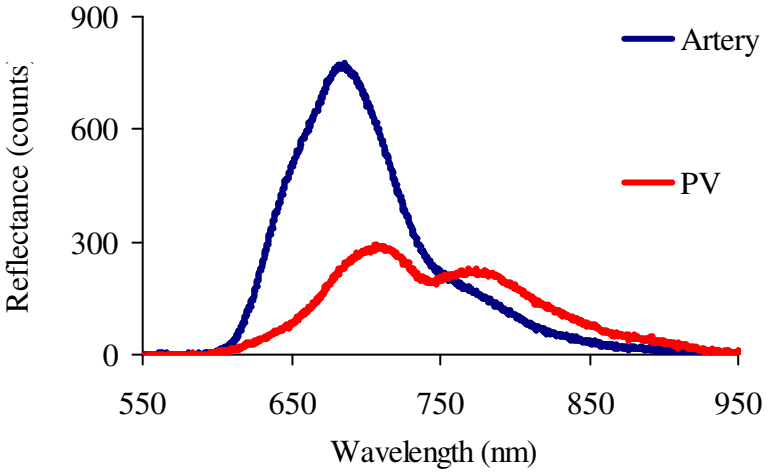

Figure 3.4 Blood Vessels

Artery's reflectance profile has a peak at 690 nm. The vein, on the other hand, contains greatly deoxy-hemoglobin. Deoxy-hemoglobin shows high absorption with reduced reflectance intensities throughout the spectral range (see fig 3.2 and fig 3.4). Vein's reflectance profile shows a peak around 700 and 800 nm. The point where the reflectance of the artery and the vein becomes equal in magnitude, is the isobestic point.

3.2 Radial Basis Function

. To show a difference in the spectra obtained from different pig biliary tract tissues, all the spectra are individually divided into three Gaussian waves. These waves, with the help of radial basis function, are made to fit the spectrum, and the components are drawn from the fit. For example, Figure 3.5 is obtained after fitting with the radial basis function to a gall spectrum. The nine parameters that are governing this fit are the amplitudes of the three Gaussian waves, their widths and centers of the Gaussian functions.

3.2.1 Biliary Tract Tissues

Biliary tract tissues are named after their major component, which is bile. These tissues include cystic duct, gall bladder, common bile duct, right hepatic duct and left hepatic duct. As the right and left hepatic duct are not much of a concern here, our measurements were taken mainly on the cystic duct, gall bladder and common bile duct.

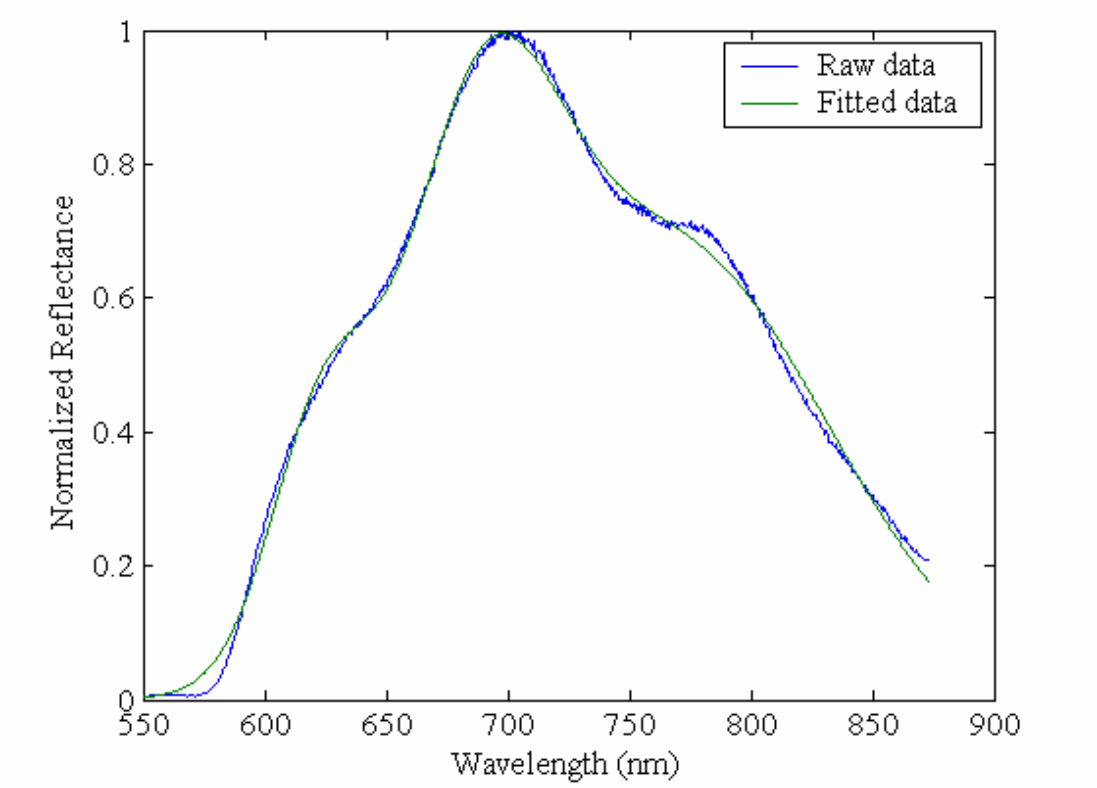

Figure 3.5 Gall spectrum fitted with the Radial Basis Function.

For figure 3.5, the R^2 of the fitted data is 1.00. The nine parameters are obtained from the fit, and they are listed in Table 3.1. In the table, a1, λ1 and σ1 represent the first Gaussian wave, a2, λ2 and σ2 represents the second Gaussian wave, and likewise for Gaussian wave 3.

Table 3.1 Nine parameters for Gall fitted data.

Organ	a_1	a_2	a_3	λ_1	λ_2	λ_3	σ_1	σ_2	σ_3
Gall	0.67	0.67	0.35	768.89	687.53	622.34	63.33	32.84	21.32

It might be cumbersome to generate a classification algorithm with all the nine

parameters. While these nine parameters are determined for all the biliary tract tissues, it may be possible to create fewer parameters to characterize the biliary tract tissues.

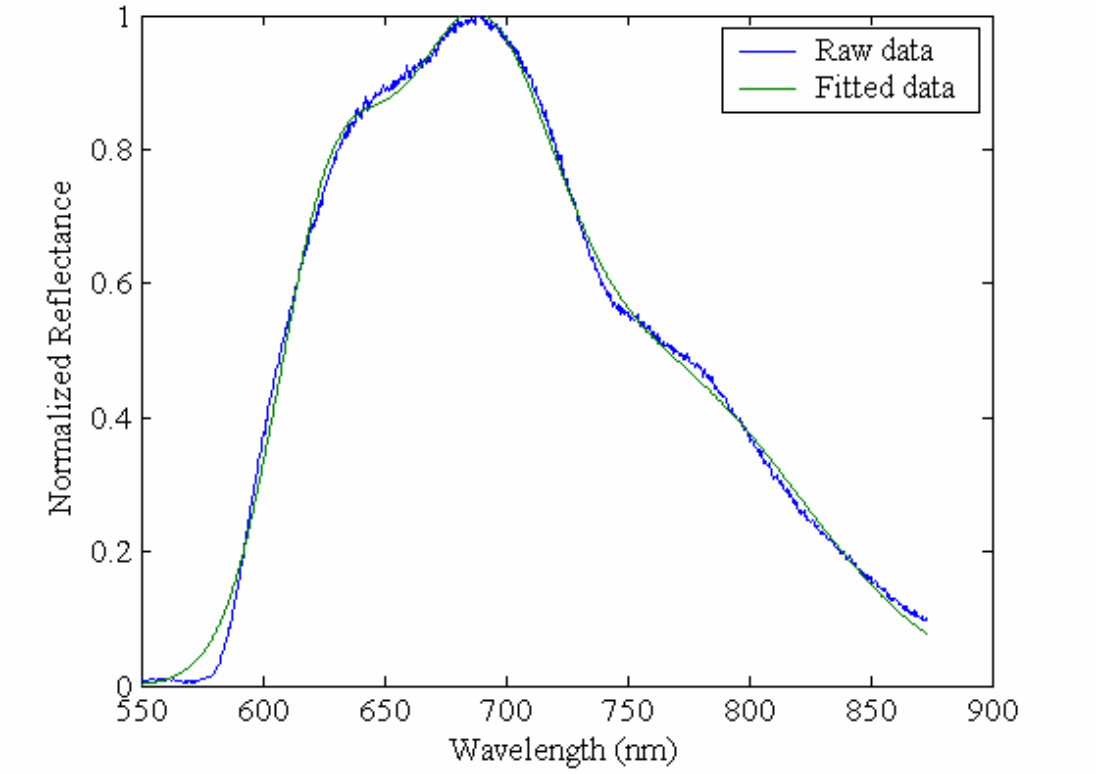

Figure 3.6 Common Bile Duct spectrum fitted with Radial Basis Function.

The above Figure 3.6 represents the fitted data for the common bile duct spectrum. The R^2 of the above fit is 1.00, which quantitatively gives us an assessment for the goodness of fit. The parameters for the above fit are given in Table 3.2.

Table 3.2 Nine governing parameters for Common Bile Duct (CBD).

Organ	a_1	a_2	a_3	λ_1	λ_2	λ_3	σ_1	σ_2	σ_3
CBD	0.44	0.85	0.51	768.53	682.68	625.10	55.50	35.77	21.73

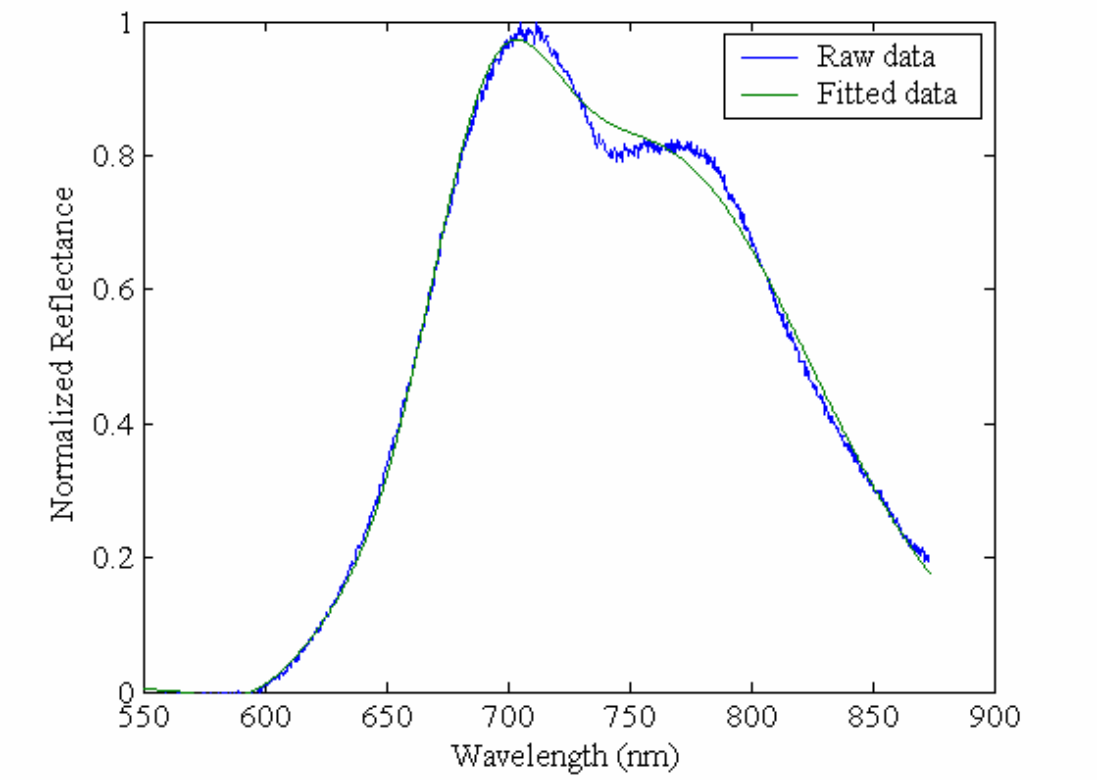

Figure 3.7 Cystic spectrum fitted with Radial Basis Function.

The fit for the Cystic duct is shown in Figure 3.7, and the nine parameters resulting this fit is given below in Table 3.3. The above fit is not as good as the Gall and the CBD, but it is still a good fit as the R^2 is 0.99.

Table 3.3 Nine governing parameters for Cystic duct.

Organ	a_1	a_2	a_3	λ_1	λ_2	λ_3	σ_1	σ_2	σ_3
Cystic	0.80	0.54	0.12	765.81	695.97	653.46	59.86	24.48	20.16

3.2.2 Blood Vessels

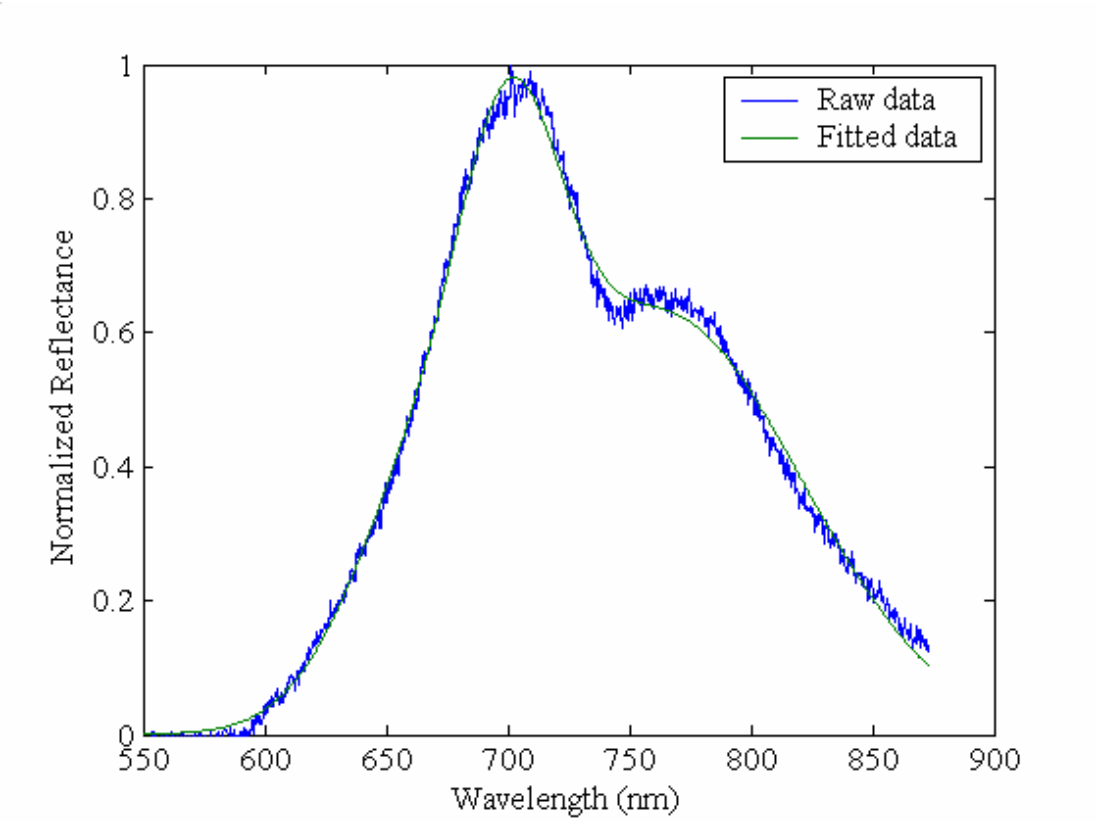

Figure 3.8 Vein spectrum fitted with Radial Basis Function.

The vein spectrum has very low amplitude and therefore is noisy when normalized to 1.0 as shown in Figure 3.8, and the fitted parameters are as listed in the Table 3.4. The R^2 of the fit is 1.00.

Table 3.4 Nine parameters obtained from the fitted data of vein spectrum.

Organ	a_1	a_2	a_3	λ_1	λ_2	λ_3	σ_1	σ_2	σ_3
vein	0.63	0.56	0.24	763.02	699.94	657.59	57.91	21.72	26.72

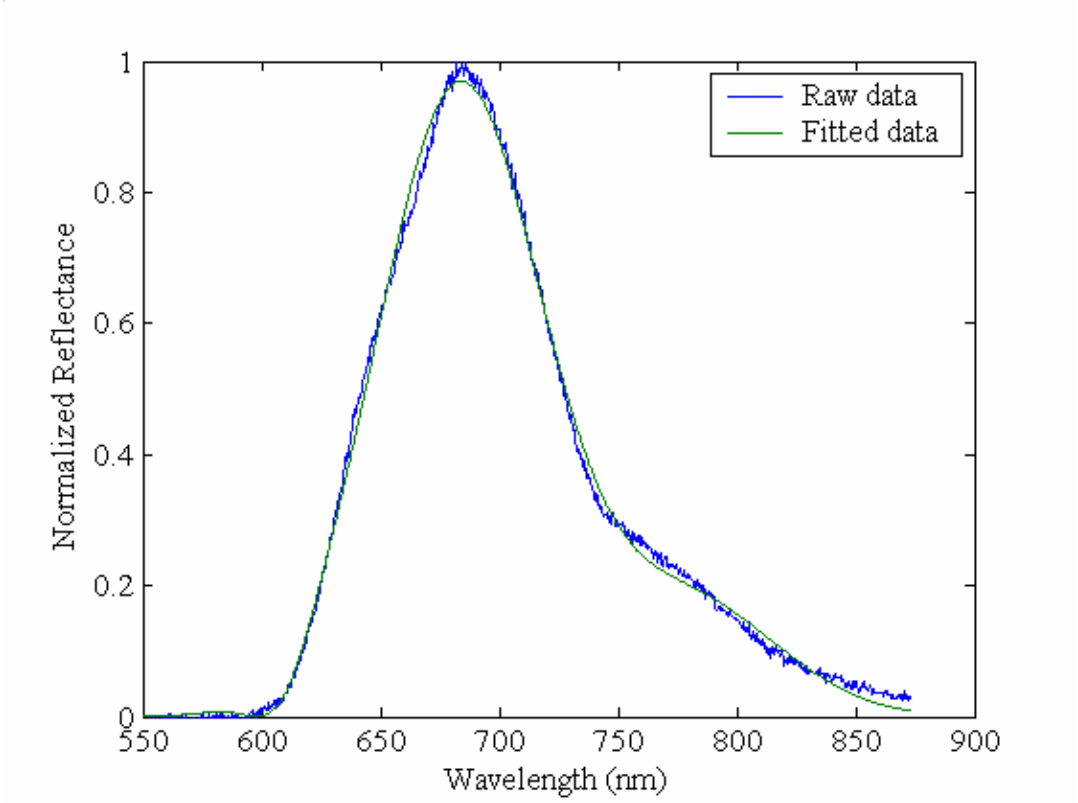

Figure 3.9 Artery spectrum fitted with Radial Basis Function.

Figure 3.9 represents the fitted data plotted with the raw data, and the parameters obtained from this fit are given below in Table 3.5. The R^2 for this fit is 0.99, which represents the goodness of the fit.

Table 3.5 Nine parameters governing the fit of the artery spectrum

Organ	a_1	a_2	a_3	λ_1	λ_2	λ_3	σ_1	σ_2	σ_3
Artery	0.18	0.96	-0.07	777.39	683.28	608.19	39.27	34.59	11.79

3.2.3 Derived Parameters

Table 3.6 represents the nine parameters obtained from the biliary tract tissue's spectra. The nine parameters represent the characteristics of the spectra of a given organ. Using all these nine parameters to differentiate between the tissues is a little tedious job. To simplify the nine parameters, further analysis was done on the nine parameters of each organ.

Table 3.6 Table representing the nine parameters of the five interested organs

Organ	a_1	a_2	a_3	λ_1	λ_2	λ_3	σ_1	σ_2	σ_3
Artery	0.18	0.96	-0.07	777.39	683.28	608.19	39.27	34.59	11.79
CBD	0.44	0.85	0.51	768.53	682.68	625.10	55.50	35.77	21.73
Cystic	0.80	0.54	0.12	765.81	695.97	653.46	59.86	24.48	20.16
Gall	0.67	0.67	0.35	768.89	687.53	622.34	63.33	32.84	21.32
Vein	0.63	0.56	0.24	763.02	699.94	657.59	57.91	21.72	26.72
Mean	0.54	0.72	0.23	768.73	689.88	633.34	55.18	29.88	20.34
S.D	0.24	0.18	0.22	5.39	7.73	21.30	9.34	6.35	5.40
% dev	43.97	25.64	94.51	0.70	1.12	3.36	16.94	21.27	26.55

Statistical analysis was done and it is found that the % deviation (= S.D/mean) for the parameters a_1, a_2, a_3, σ_2 and σ_3 is greater than the other parameters (> 20%). This explains that a_1, a2, a_3, σ_2 and σ_3 can be used as significant classifiers to differentiate between the organs that are specified in the Table 3.6. To make it simpler, three parameters are derived from a_1, a_2, a_3, σ_2 and σ_3. As aforementioned a_1, a_2 and a_3 represents the amplitudes of three Gaussian's and A=(a_1/ a_2), B=(a_3/ a_2)will give us the ratio of as how the amplitudes of the first and the third Gaussian will change with respect to the middle or the second Gaussian.

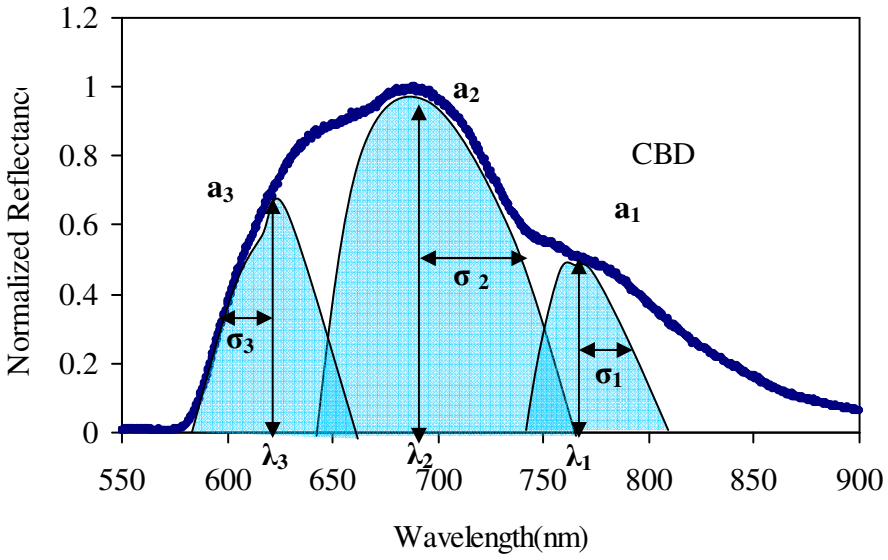

Figure 3.10 The three Gaussian waves from the Radial basis function.

Similarly, as shown in figure 3.10, C= (σ_2/ σ_3) is the ratio of the middle or second Gaussian to the third Gaussian. From Table 3.6, it is shown that these 5 parameters (a_1, a2, a_3, σ_2 and σ_3) show a greater deviation than λ_1, λ_2, λ_3 and σ_1, thus

allowing us to choose A, B and C as the derived parameters. The derived parameters for Pig-1 measurements are as shown in table 3.7.

Table 3.7 A, B and C Parameters for Pig-1

Organ	**A**	**B**	**C**
Artery	0.19	-0.07	0.34
CBD	0.52	0.60	0.61
Cystic	1.47	0.23	0.82
Gall	1.01	0.52	0.65
Vein	1.12	0.43	1.23

3.3 Pig Measurements

After Pig-1, experiments were performed on seven more live pigs, and the parameters A, B and C were derived out of the reflectance measurements.

3.3.1 Pig-2 Measurements

The reflectance measurements for Pig-2 are as shown in figure 3.11. The integration time is not maintained constant to get a good reflectance signal. The spectra are normalized for all the organs during their fitting with Radial Basis Function.

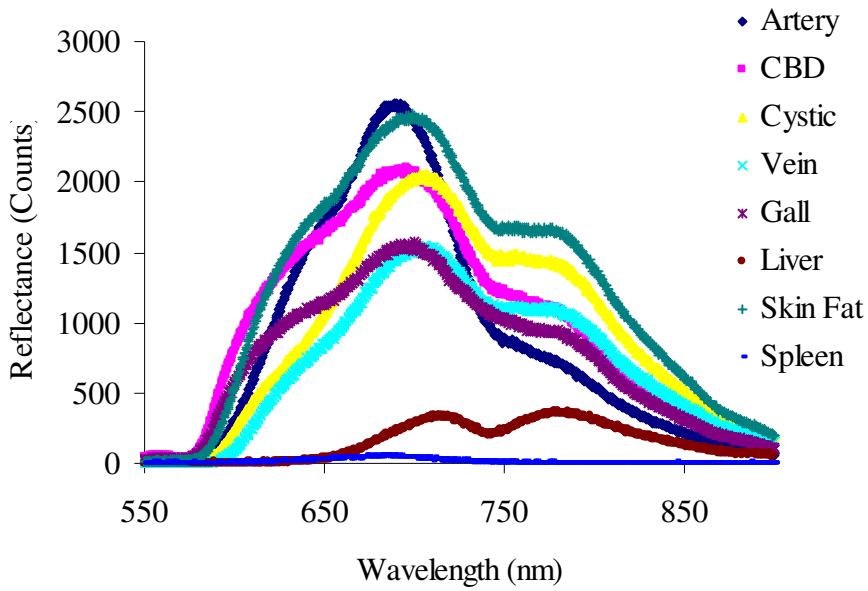

Figure 3.11 Pig-2 Measurements.

The reflectance spectra from the biliary tract tissues and the blood vessels are shown in figure 3.12

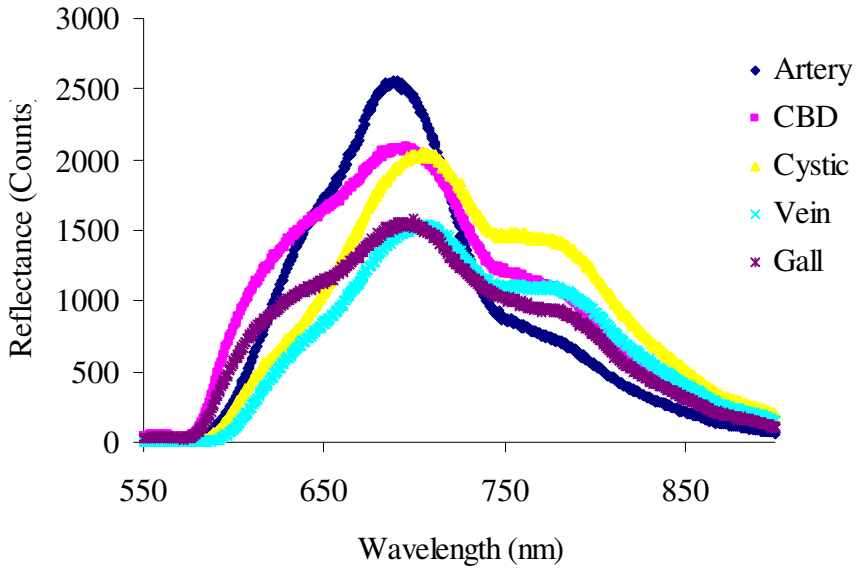

Figure 3.12 Biliary tract tissues and the blood vessels Spectra.

These spectra are fitted with Radial basis function as aforementioned in Section 3.2. The nine parameters for the biliary tree and the blood vessels for pig-2 are given in table 3.8.

Table 3.8 Nine parameters from the spectra obtained from Pig-2

Organ	a_1	a_2	a_3	λ_1	λ_2	λ_3	σ_1	σ_2	σ_3
Artery	0.20	0.95	-0.05	820.35	697.23	590.85	36.92	46.22	12.68
CBD	0.48	0.84	0.48	789.93	699.47	631.35	57.61	36.68	24.63
Cystic	0.87	0.44	0.27	795.23	719.62	683.56	59.39	22.00	32.79
Gall	0.56	0.77	0.46	787.77	698.92	630.42	58.87	36.03	24.08
Vein	0.69	0.66	0.33	787.24	707.65	648.67	62.14	28.67	22.84
Mean	0.56	0.73	0.30	796.10	704.58	636.97	54.99	33.92	23.40
S.D	0.25	0.20	0.22	13.92	9.33	33.57	10.23	9.12	7.16
% deviation	44.98	26.58	72.24	1.75	1.32	5.27	18.61	26.90	30.61

A, B and C parameters for Pig-2 are listed in table 3.9.

Table 3.9 A, B and C Parameters for Pig-2

Organ	A	B	C
Artery	0.21	-0.05	0.27
CBD	0.57	0.57	0.67
Cystic	1.98	0.60	1.49
Gall	0.73	0.59	0.67
Vein	1.04	0.50	0.80

3.3.2 Pig-3 Measurements

The reflectance measurements obtained from pig-3 are as shown in figure 3.13.

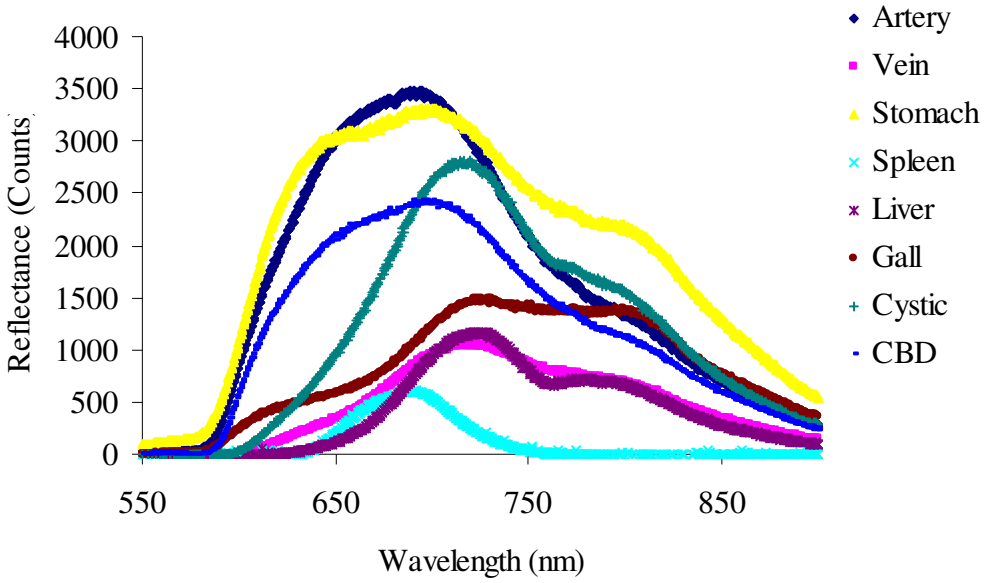

Figure 3.13 Pig-3 Measurements.

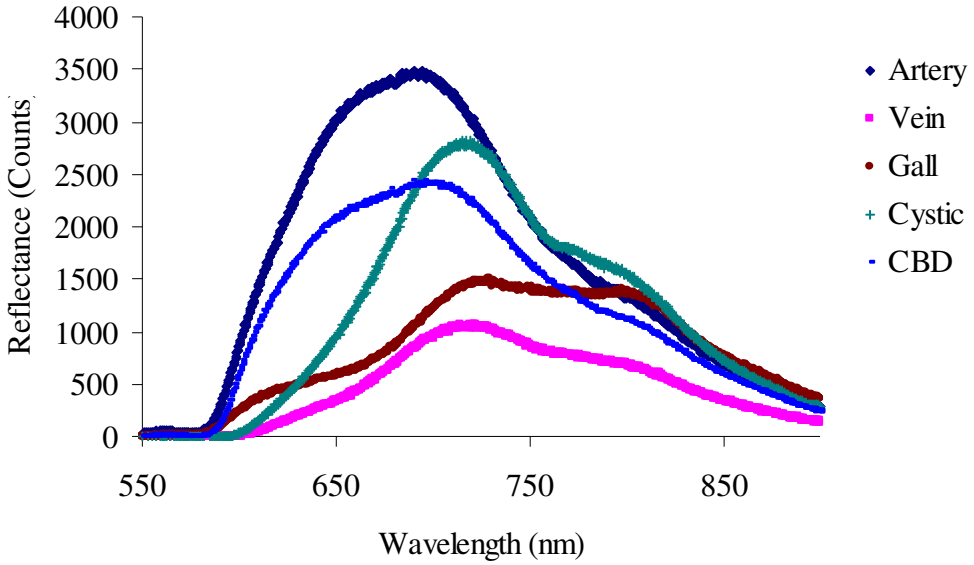

Figure 3.14 Biliary tree and blood vessels measurements on Pig-3.

The artery measurement in this case is taken on the spleenic artery and has a few millimeters of fat embedded on it. The biliary tree measurements and the blood vessels measurement are shown in figure 3.14. In this pig's case, the gall shows a different profile than what we have observed in pig-1 and pig-2. The nine parameters for these obtained spectra are listed in table 3.10. A, B and C parameters for pig-3 are listed in table 3.11.

Table 3.10 Nine Parameters obtained from the spectra of Pig-3 organs.

Organ	a_1	a_2	a_3	λ_1	λ_2	λ_3	σ_1	σ_2	σ_3
Artery	0.39	0.80	0.39	775.51	688.92	632.73	66.51	39.15	23.85
CBD	0.46	0.79	0.43	777.23	689.89	631.22	66.09	39.65	22.26
Cystic	0.46	0.86	-0.02	799.31	707.13	590.47	51.34	40.54	9.21
Gall	0.91	0.38	0.26	781.14	709.02	634.21	68.43	26.27	26.72
Vein	0.57	0.73	-0.02	791.60	706.47	582.89	58.47	40.47	15.10
Mean	0.56	0.71	0.21	784.96	700.29	614.30	62.17	37.22	19.43
S.D	0.21	0.19	0.22	10.17	9.98	25.38	7.15	6.15	7.14
% deviation	37.73	26.88	104.98	1.30	1.43	4.13	11.50	16.52	36.75

Table 3.11 A, B and C Parameters of Pig-3.

Organ	**A**	**B**	**C**
Artery	0.48	0.49	0.61
CBD	0.58	0.55	0.56
Cystic	0.53	-0.02	0.23
Gall	2.40	0.68	1.02
Vein	0.78	-0.03	0.37

3.3.3 Pig-4 Measurements

The reflectance measurements of pig-4 are shown in figure 3.15.

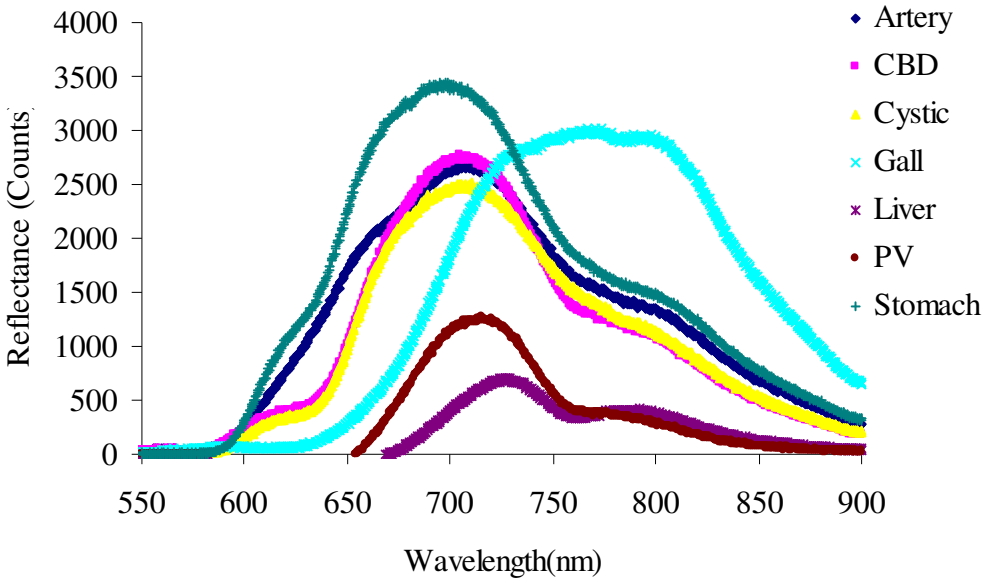

Figure 3.15 Pig-4 Measurements

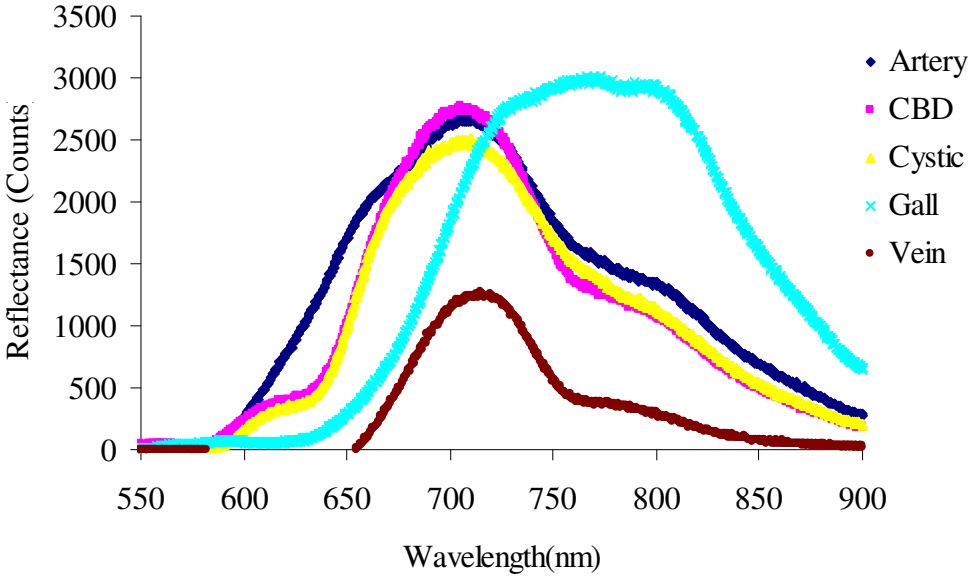

Figure 3.16 Biliary tree and blood vessels spectra of Pig-4

Figure 3.16 shows the reflectance spectra obtained from the five interested organs, i.e. Cystic Duct, Artery, Common Bile Duct (CBD), Vein and Gall. The Gall spectrum shows a different profile when compared to pig-1. The vein spectrum in this case is the measurement taken from portal vein. The portal vein is generally underneath the common bile duct which itself is embedded in a few millimeters of fat. The measurement therefore includes the fat, common bile duct and the portal vein. The first separation of the probe is 0.95 cm, which gathers reflectance from a few millimeters deep in tissue. The nine parameters obtained from the fitted spectra of pig-4 are listed in table 3.12.

Table 3.12 Nine Parameters obtained from Pig-4 Spectra of biliary tract tissues.

Organ	a_1	a_2	a_3	λ_1	λ_2	λ_3	σ_1	σ_2	σ_3
Artery	0.36	0.94	-0.06	811.25	697.24	590.59	50.74	50.46	15.43
CBD	0.37	0.88	0.08	783.30	698.19	608.46	57.65	35.28	11.83
Cystic	0.47	0.77	0.06	771.38	695.65	609.17	63.45	35.46	7.73
Gall	0.97	0.29	0.02	784.83	718.13	582.37	62.20	25.75	14.21
Vein	0.23	0.98	-0.16	788.66	711.29	629.94	35.89	26.97	24.48
Mean	0.48	0.77	-0.01	787.89	704.10	604.11	53.99	34.78	14.74
S.D	0.29	0.28	0.10	14.57	10.03	18.49	11.27	9.86	6.19
% deviation	59.98	36.21	803.04	1.85	1.42	3.06	20.88	28.36	42.00

A, B, C Parameters of Pig-4 are listed in Table 3.13.

Table 3.13 A, B, C Parameters of Pig-4

Organ	**A**	**B**	**C**
Artery	0.38	-0.06	0.31
CBD	0.42	0.09	0.34
Cystic	0.62	0.07	0.22
Gall	3.32	0.06	0.55
Vein	0.23	-0.16	0.91

3.3.4 Pig-5 Measurements

The reflectance measurements were taken only on the biliary tract tissues and on artery in case of pig-5. Figure 3.17 shows us that the gall is showing a profile, similar to that of pig-1.The artery measurement, is taken from the spleenic artery. The nine parameters for the four organs measured in pig-5 are listed in table 3.17.

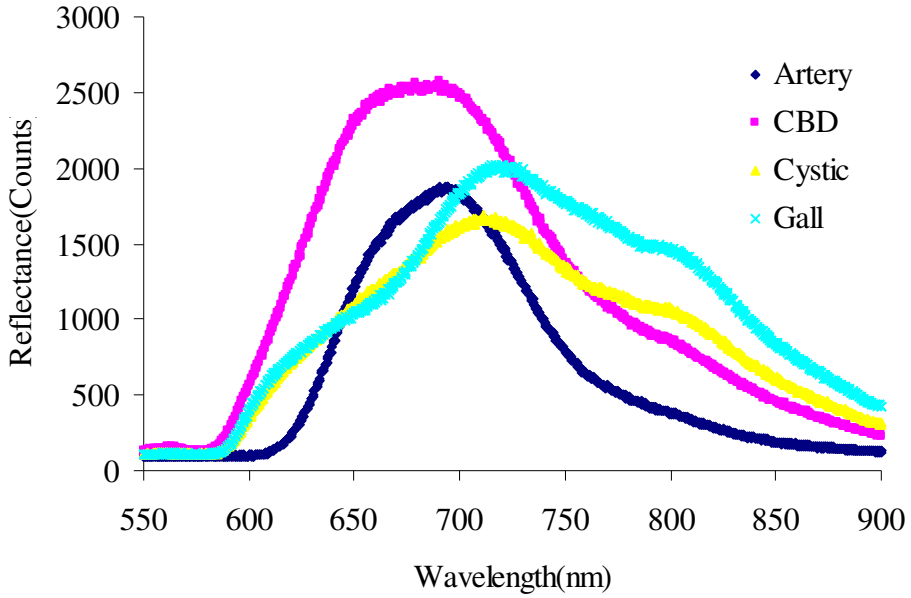

Figure 3.17 Pig-5 Measurements

Table 3.14 Nine parameters obtained from the fitted data of Pig-5.

Organ	a_1	a_2	a_3	λ_1	λ_2	λ_3	σ_1	σ_2	σ_3
Artery	0.22	0.80	-0.16	737.05	687.22	617.10	95.89	38.80	16.49
CBD	0.35	0.72	0.29	756.87	685.62	637.73	82.76	39.94	23.00
Cystic	0.46	0.84	0.03	805.93	693.09	553.07	63.66	56.43	5.77
Gall	0.78	0.35	0.23	763.88	706.59	632.12	80.22	28.88	23.10
Mean	0.45	0.68	0.10	765.93	693.13	610.00	80.63	41.01	17.09
S.D	0.24	0.22	0.20	28.98	9.53	38.95	13.24	11.42	8.16
***%* deviation**	52.13	32.79	210.14	3.78	1.37	6.38	16.42	27.84	47.73

A, B and C parameters for the four organs of Pig-5 are as listed in table 3.15.

Table 3.15 A, B and C Parameters of Pig-5 Measurements.

Organ	**A**	**B**	**C**
Artery	0.28	-0.20	0.43
CBD	0.49	0.40	0.58
Cystic	0.55	0.03	0.10
Gall	2.20	0.66	0.80

3.3.5 Pig-6 Measurements

The measurements taken on the organs of pig-6 are shown in figure 3.16. The only other abdominal tissue measurement that was taken in this case was liver.

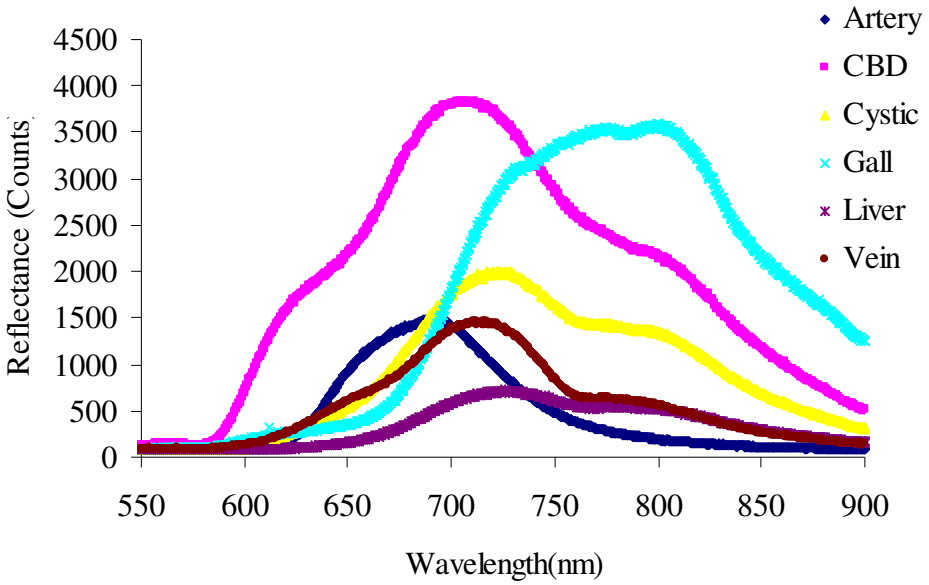

Figure 3.18 Pig-6 Measurements.

The reflectance profile of gall is similar to that of pig-3 and pig-4. Figure 3.18 depicts that the biliary tract tissues have the same reflectance to that of pig-1. Cystic duct is about 3millimeters in width and as it is attached to the liver, there is a high possibility of the probe detecting the liver too in the cystic reflectance profile. The biliary tract tissues and the blood vessels reflectance spectra are shown in figure 3.18.

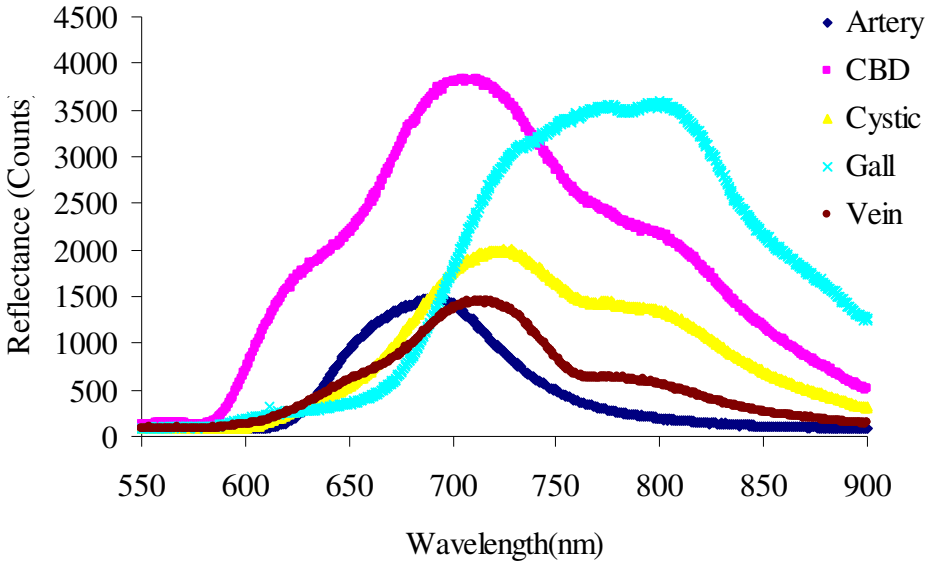

Figure 3.19 Biliary tract tissues and blood vessels of Pig-6.

The nine parameters, which have resulted from the fit provided by the radial basis function, are tabulated in table 3.16.

Table 3.16 Nine Parameters from the spectra of the biliary tract tissues of Pig-6.

Organ	a_1	a_2	a_3	λ_1	λ_2	λ_3	σ_1	σ_2	σ_3
Artery	0.16	0.83	-0.14	728.57	685.68	620.04	106.28	35.63	15.76
CBD	0.32	0.95	-0.09	828.51	705.01	583.76	45.27	59.98	9.75
Cystic	0.68	0.44	0.11	773.07	711.37	670.34	68.79	26.04	46.27
Gall	0.96	0.24	0.04	792.56	726.99	600.97	66.34	23.67	26.60
Vein	0.44	0.52	0.23	745.59	715.75	672.40	82.22	21.16	28.45
Mean	0.51	0.60	0.03	773.66	708.96	629.50	73.78	33.30	25.37
S.D	0.32	0.29	0.15	39.33	15.29	40.33	22.48	15.89	14.00
***%* deviation**	62.01	48.47	505.78	5.08	2.16	6.41	30.46	47.73	55.20

The derived parameters A, B and C are listed in table 3.17.

Table 3.17 A, B and C Parameters of Pig-6.

Organ	**A**	**B**	**C**
Artery	0.19	-0.17	0.44
CBD	0.33	-0.09	0.16
Cystic	1.55	0.25	1.78
Gall	4.02	0.17	1.12
Vein	0.85	0.44	1.34

3.3.6 Pig-7Measurements

Figure 3.20 represents the reflectance profiles from the tissues of Pig-7. The reflectance profile of stomach is different as compared to that of pig-1.

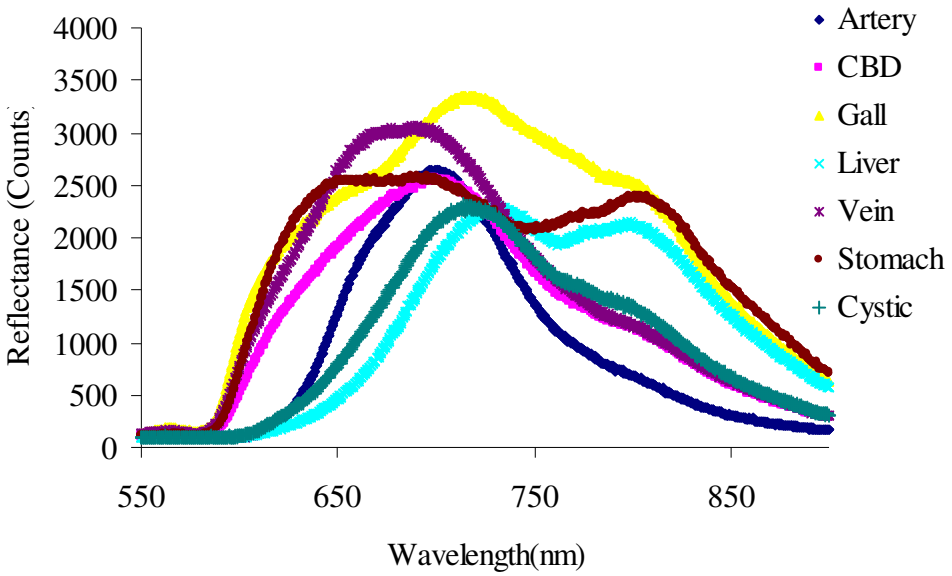

Figure 3.20 Pig-7 Measurements.

Gall, CBD and Artery have a consistent profile with the reflectance measurements on pig-1. The vein measurement was taken on the renal vein, which had up to 2 millimeters of fat on it. Figure 3.21 represents the biliary tree organs and the blood vessels.

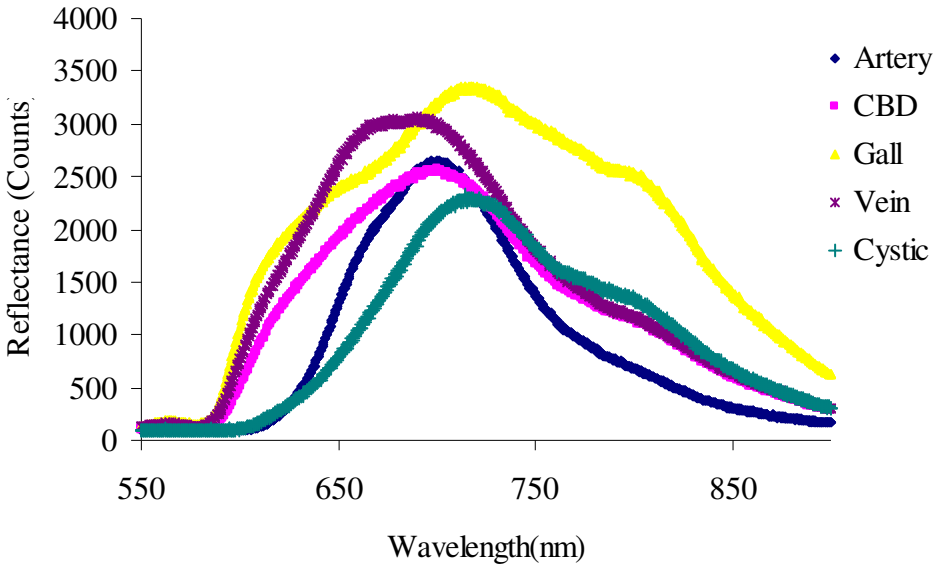

Figure 3.21 Biliary tree measurements on Pig-7.

The nine parameters for each organ, when fitted with radial basis function, are listed below in table 3.18.

Table 3.18 Nine Parameters derived from the spectra measured on Pig-7

Organ	a_1	a_2	a_3	λ_1	λ_2	λ_3	σ_1	σ_2	σ_3
Artery	0.31	0.71	-0.11	737.65	695.22	619.30	737.65	695.22	619.30
CBD	0.45	0.73	0.27	769.76	689.56	629.17	73.54	39.84	21.44
Cystic	0.60	0.50	0.02	763.73	705.06	614.80	73.39	32.79	135.42
Gall	0.74	0.59	0.40	779.68	692.95	625.57	68.65	41.19	23.17
Vein	0.38	0.76	0.27	770.33	685.52	633.01	74.49	41.29	25.71
Mean	0.50	0.66	0.17	764.23	693.66	624.37	205.55	170.06	165.01
S.D	0.17	0.11	0.21	15.91	7.35	7.36	297.47	293.59	258.55
% deviation	34.78	17.18	123.06	2.08	1.06	1.18	144.72	172.64	156.69

In table 3.18, the percentage deviation of a2 is less than σ_1, which is different from the other seven pigs. Table 3.19 represents the derived parameters A, B and C from the nine parameters for Pig-7.

Table 3.19 A, B and C Parameters of Pig-7.

Organ	**A**	**B**	**C**
Artery	0.44	-0.16	0.89
CBD	0.61	0.37	0.54
Cystic	1.21	0.03	4.13
Gall	1.26	0.69	0.56
Vein	0.50	0.35	0.62

3.3.7 Pig-8 Measurements

Figure 3.22 plots the reflectance measurements taken on the biliary tree, blood vessels and liver from Pig-8. The profile of liver shows that it was less de-oxy than the other pigs (Pig-1 to Pig-7).

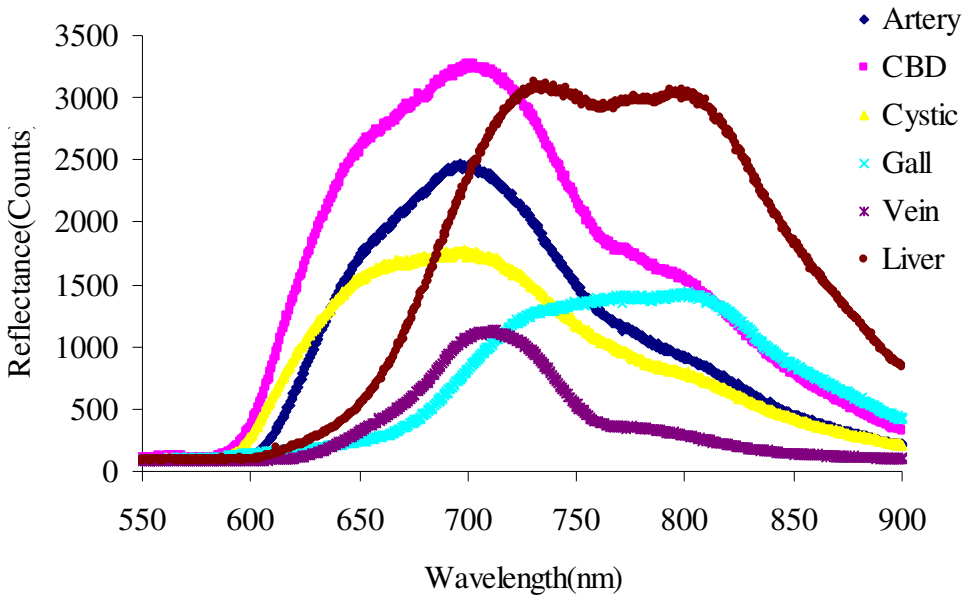

Figure 3.22 Pig-8 Measurements

Gall exhibits a profile which is similar to pig-3, but not to pig-1. Figure 3.23 plots all the biliary tract tissues of pig-8.

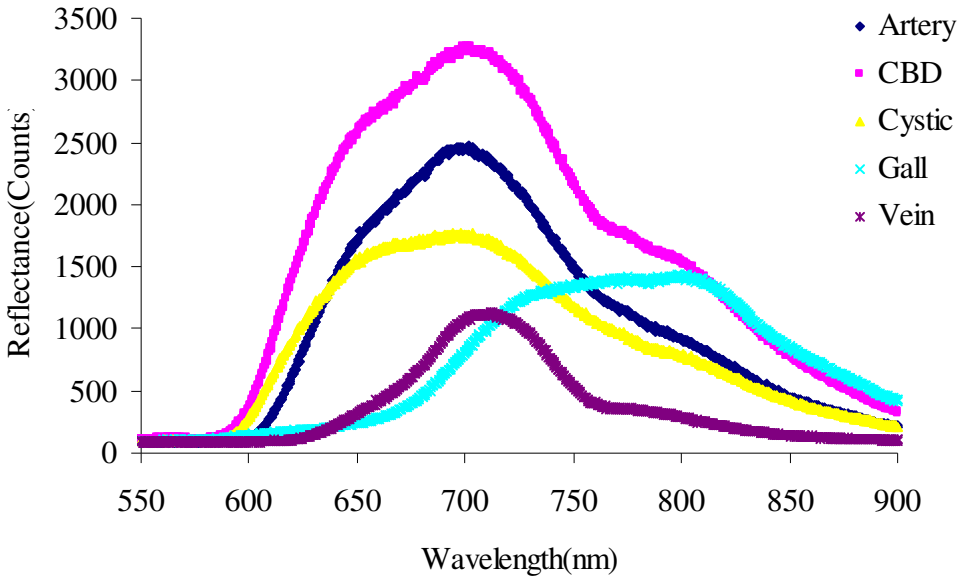

Figure 3.23 Biliary tree tissues of Pig-8.

The nine parameters resulted from the above raw spectra are listed below in table 3.20, and the derived parameters of A, B and C are given in table 3.21.

Table 3.20 Table representing the nine parameters derived from Pig-8 spectra.

Organ	a_1	a_2	a_3	λ_1	λ_2	λ_3	σ_1	σ_2	σ_3
Artery	0.26	0.94	0.14	806.76	691.23	604.62	55.09	49.88	14.41
CBD	0.50	0.65	0.51	766.40	699.99	642.57	71.33	31.47	23.68
Cystic	0.29	0.95	0.24	806.00	680.01	591.51	64.60	60.06	18.54
Gall	0.98	0.19	0.08	785.83	721.30	592.22	68.43	20.50	41.79
Vein	0.29	0.69	0.06	754.92	710.53	666.98	83.55	25.54	107.40
Mean	0.47	0.68	0.05	783.98	700.61	619.58	68.60	37.49	41.17
S.D	0.30	0.31	0.29	23.24	16.12	33.67	10.36	16.81	38.47
% deviation	65.25	45.06	55.30	2.96	2.30	5.43	15.11	44.84	93.46

Table 3.21 A, B and C parameters of Pig-8 measurements.

Organ	**A**	**B**	**C**
Artery	0.28	-0.15	0.29
CBD	0.77	0.78	0.75
Cystic	0.31	-0.26	0.31
Gall	5.10	0.40	2.04
Vein	0.42	0.09	4.20

3.4 Statistical Analysis

Statistical analysis is done on the biliary tract tissues and the blood vessels of all the eight live pigs. This analysis is performed to check the consistency of the derived parameters. If the data are consistent among all eight pigs, then these derived parameters can be assigned a certain range of values and used for differentiation between the biliary tract tissues.

3.4.1Comparing Pig Spectra

Pig spectra are compared by normalizing the data to 1.0. Reflectance measurements of pig-1 are considered as the standard profile. Spectrum profiles of pigs from 2 to 8 are compared to that of pig-1.

3.4.1.1 Artery

Figure 3.24 plots the artery spectra of pigs 1 to 8. Artery profiles from the eight pigs are quite consistent as shown in Figure 3.24 with Artery-3 and Artery-4 being exceptions. Artery-3 (pig-3) is not of a close match with the other pigs as the measurement was taken on the renal artery, which had relatively a greater thickness of fat than the other pig's, measurements that were taken on the spleenic, or the stomach artery. Artery-4 is showing a peak near 800nm, which might be due to noise from other tissues as most of them are quite close to one another. The source-detector separation is 0.95 cm and is more susceptible to pick up noise from the other tissues.

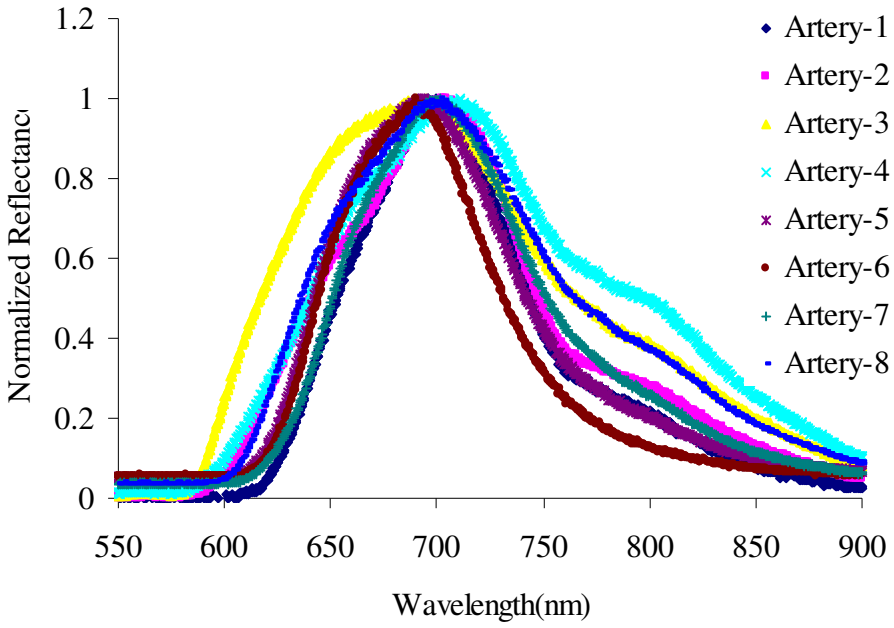

Figure 3.24 Artery spectra

3.4.1.2 Common Bile Duct

Common bile duct (CBD) spectra from pigs 1 to 8 are plotted in figure 3.25. Spectra from pigs 2,3,7 and 8 are quite consistent with Pig-1. CBD-4 shows us a different profile. CBD-6 shows an added feature of gall in its spectrum, which might be because bile is the major component in these organs and the bile-like signature can be shown in the biliary tissues. CBD-5 has a shifted peak at around 670 nm.

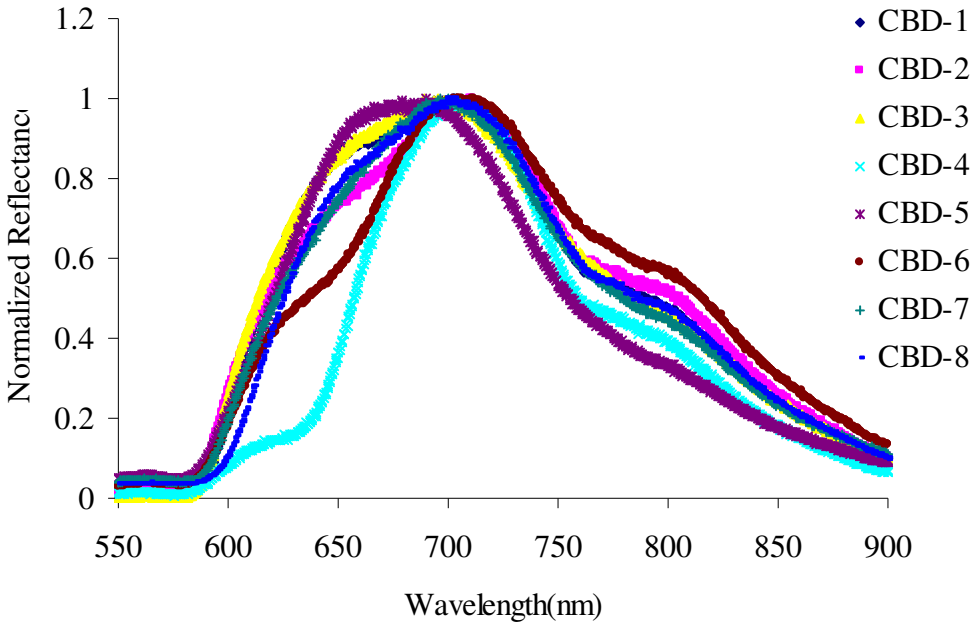

Figure 3.25 Common Bile Spectra

3.4.1.3 Cystic duct

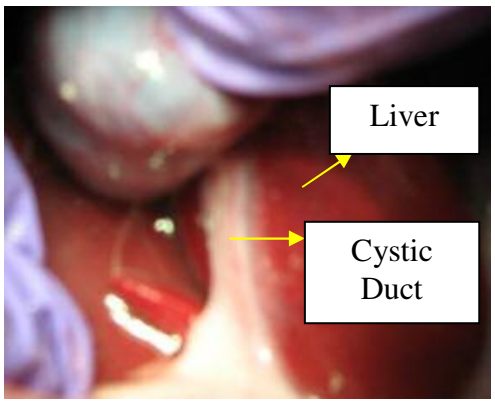

Figure 3.26 Cystic duct and Liver

Cystic duct is smaller in thickness as compared to that of humans. As the probe can collect the reflectance from a tissue, which is 5 mm deep, there is a high probability that the cystic data is contaminated with liver reflectance (see Figure 3.26). Figure 3.27

plots the cystic spectra obtained from pigs 1 to 8. The peaks near 800 nm for all the pig's cystic spectra are different in amplitude due to varying noise from the liver. Cystic-8 shows a shifted peak and is not consistent with that of pig-1.

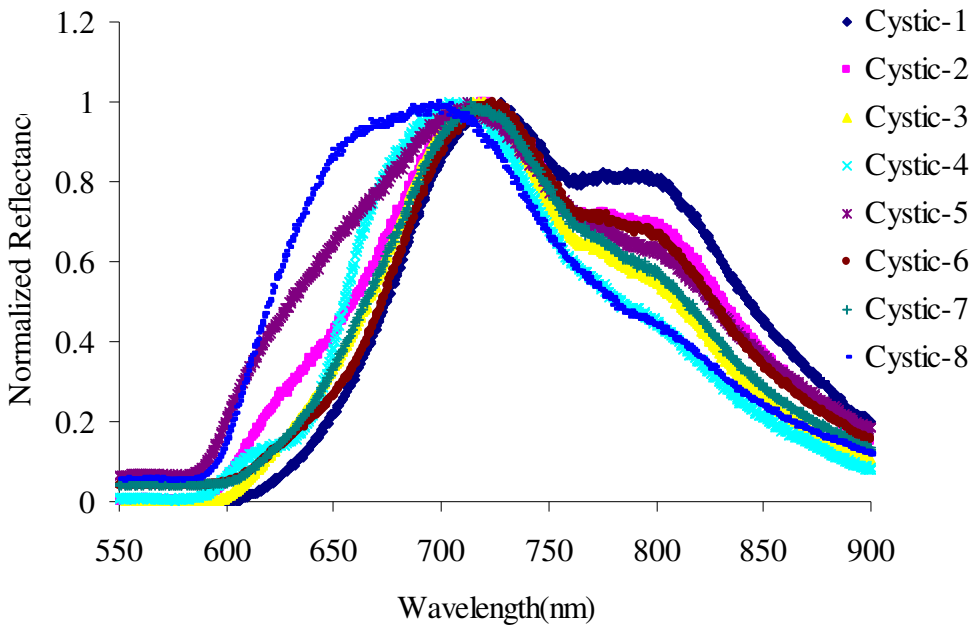

Figure 3.27 Cystic Duct Spectra

3.4.1.4 Gall Bladder

Figure 3.28 shows us the Gallbladder spectra obtained from the in vivo readings of all eight pigs. From this figure, it is quite clear that gall exhibits two kinds of profiles. Pigs 2, 7 and 5 exhibits consistency with pig-1, whereas pigs 6 and 8 exhibit different, but consistent spectra with pig-4. Gall-3 shows a mixed profile: it is consistent with pig-1 until 700 nm, and then consistent with pig-4 until 900nm.

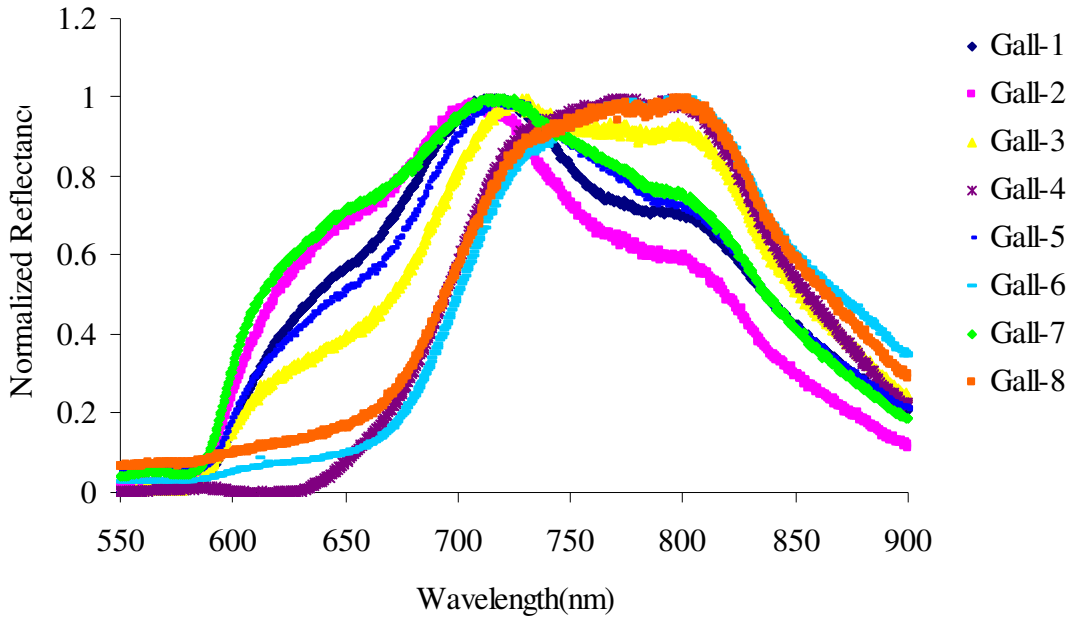

Figure 3.28 Gall Bladder Spectra

3.4.1.5 Vein

Figure 3.29 plots the vein spectra measured in vivo on seven pigs. In the case of Pig-5, vein's measurement was not available. From figure 3.29, we can see two kinds of profiles. Pigs 1, 2 and 3 have a peak with higher amplitude at 800 nm. Pigs 6,7 and 8 show a peak with less amplitude when compared to that of pig-1. Pig-4's vein spectrum shows huge absorption until 650 nm.

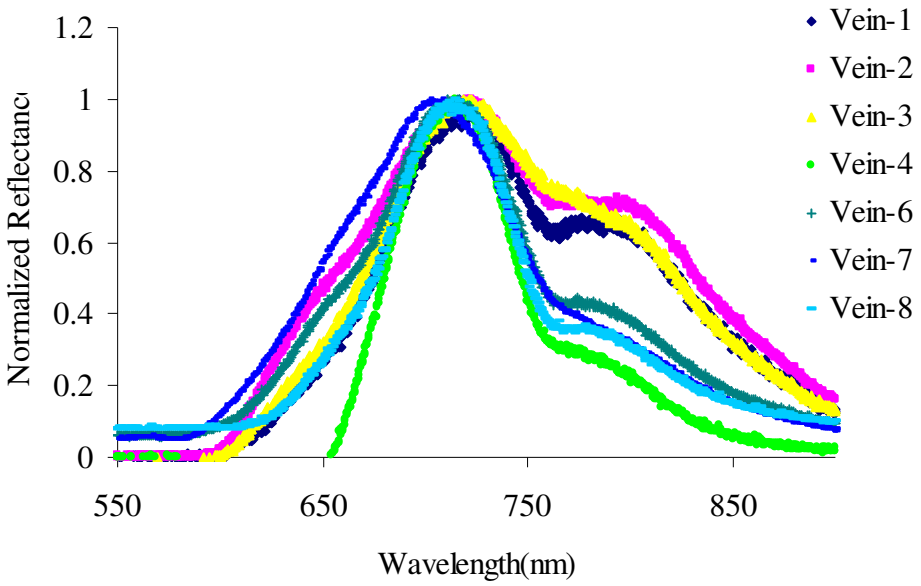

Figure 3.29 Vein Spectra

3.4.2 Statistics

The derived parameters obtained by fitting the radial basis function and then reducing them to A, B and C offers a way to classify biliary tract tissues and blood vessels. As aforementioned, if the parameters A, B and C are consistent over their respective organs, they could be good classifiers to differentiate the biliary tree and blood vessels. A statistical approach is used with all the in vivo data obtained from the eight pigs. Table 3.22 lists the statistics made on the artery data. Artery-4 was not considered, as it was not consistent with the other pigs as discussed in section 3.4.1.1. Figure 3.30 depicts the mean value of the parameters A, B and C over seven pigs and the error bars represent their standard error of mean. From figure 3.30 and table 3.22, it

is observed that parameters A, B and C are consistent over the seven pigs taken into consideration.

Table 3.22 Artery data

Organ	**A**	**B**	**C**
Artery-1	0.19	-0.07	0.34
Artery-2	0.21	-0.05	0.27
Artery-3	0.48	-0.49	0.61
Artery-5	0.28	-0.20	0.43
Artery-6	0.29	-0.17	0.44
Artery-7	0.44	-0.16	0.89
Artery-8	0.28	-0.15	0.29
Mean	0.31	-0.18	0.47
S.D	0.11	0.14	0.22
SEM	0.04	0.05	0.08

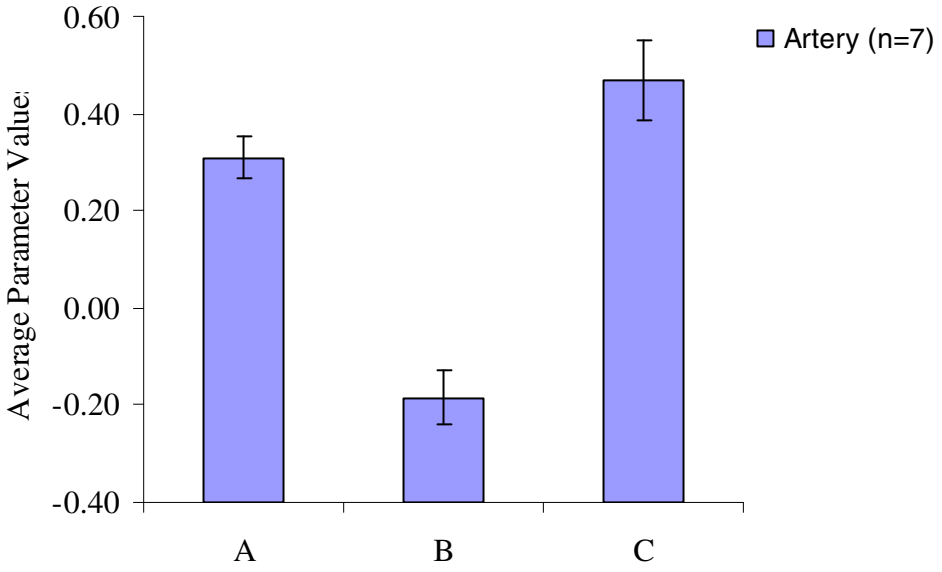

Figure 3.30 A, B and C parameters of Artery data with SEM as error bars.

Table 3.23 and figure 3.31 represents the data taken on the Common Bile Duct (CBD). The mean and standard error of mean (SEM) of the parameters A, B and C are obtained by taking in vivo readings on six of the eight pigs. The spectra obtained from pig-6 and pig-4 are not taken into consideration as explained in section 3.4.1.2 for the reasons of not being consistent with other pigs. Figure 3.31 represents the average values of the parameters with standard error of mean as the error bars. The data is consistent with a SEM less than 7 percent.

Table 3.23 CBD data

Organ	A	B	C
CBD-1	0.52	0.60	0.61
CBD-2	0.57	0.57	0.67
CBD-3	0.58	0.55	0.56
CBD-5	0.49	0.40	0.58
CBD-7	0.61	0.37	0.54
CBD-8	0.77	0.78	0.75
MEAN	0.59	0.55	0.62
S.D	0.10	0.15	0.08
SEM	0.04	0.06	0.03

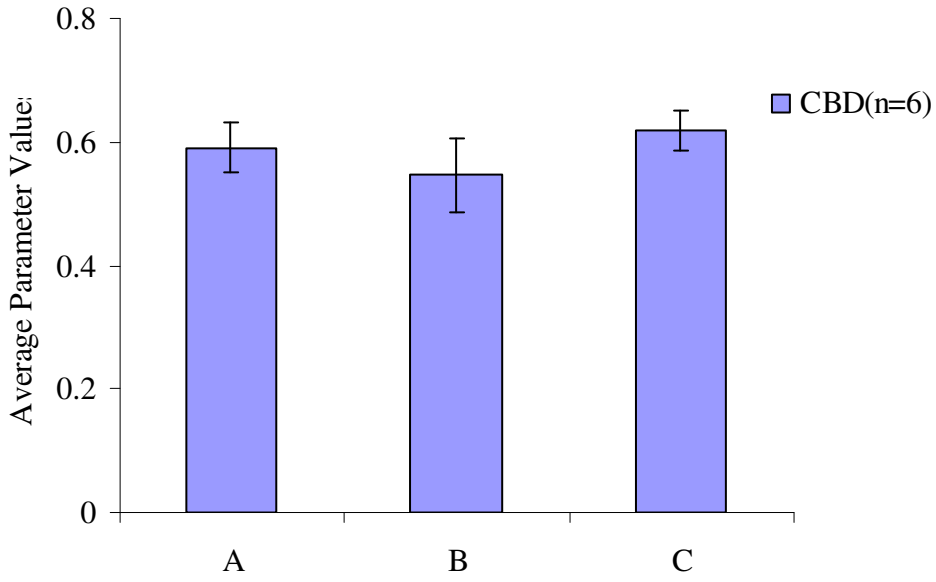

Figure 3.31 Average A, B and C Parameters with SEM as their error bars.

Table 3.24 lists the statistics of the data taken on the cystic duct. As aforementioned, pig-7 and pig-8 are not considered. The data is thus from the remaining six pigs (n=6). Cystic duct is a very thin duct in pigs; however, it is relatively bigger in humans. As the cystic duct is very thin, it is more susceptible to noise. Pig-7 and Pig-8 are considered noisy when compared to the other pigs data.

Table 3.24 Cystic duct data

Organ	A	B	C
Cystic-1	1.47	0.23	0.82
Cystic-2	1.98	0.60	1.49
Cystic-3	0.53	0.02	0.23
Cystic-4	0.62	0.07	0.22
Cystic-5	0.55	0.03	0.10
Cystic-6	1.55	0.25	1.78
MEAN	1.12	0.20	0.77
S.D	0.63	0.22	0.72
SEM	0.26	0.09	0.29

Figure 3.32 plots the average values of the six pig's derived parameters for the cystic duct. The SEM is relatively larger than those from the other organs.

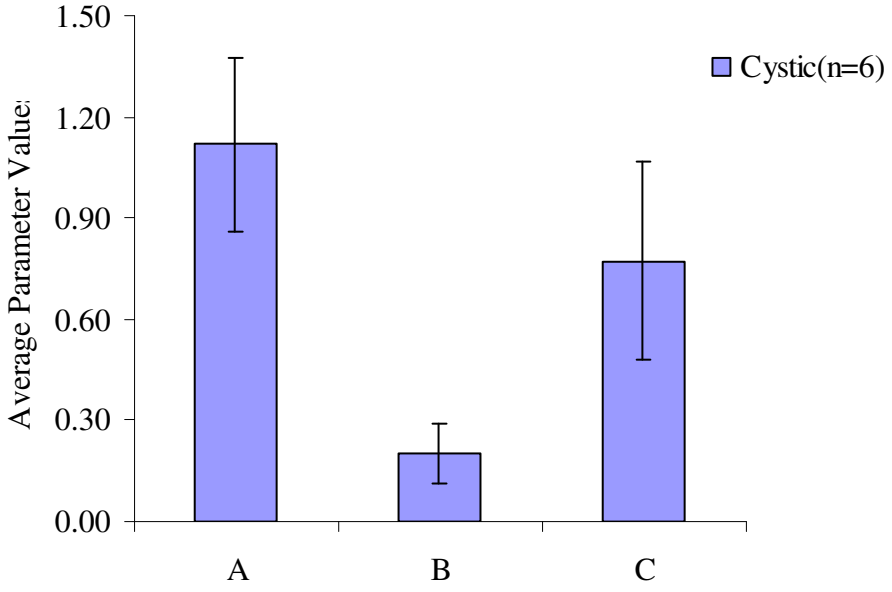

Figure 3.32 Average values of Parameters A, B and C with SEM as error bars.

In section 3.4.1.4, it is mentioned that Gall had been observed as having two different kinds of profiles, and pigs 1,2,5 and 7 have shown different profiles when compared to pigs 3, 4, 6 and 8. Therefore, the gall data are split into Gall-1 and Gall-2. Table 3.25 lists the average values of Gall-1 with SEM. Figure 3.33 gives us the graphical representation of the data from table 3.25. The SEM of the parameters A, B and C are represented as the error bars.

Table 3.25 Gall-1 data

Organ	A	B	C
Gall-1	1.01	0.52	0.65
Gall-2	0.73	0.59	0.67
Gall-5	1.20	0.66	0.80
Gall-7	1.26	0.69	0.56
MEAN	1.05	0.62	0.67
STDEV	0.24	0.08	0.10
SEM	0.12	0.04	0.05

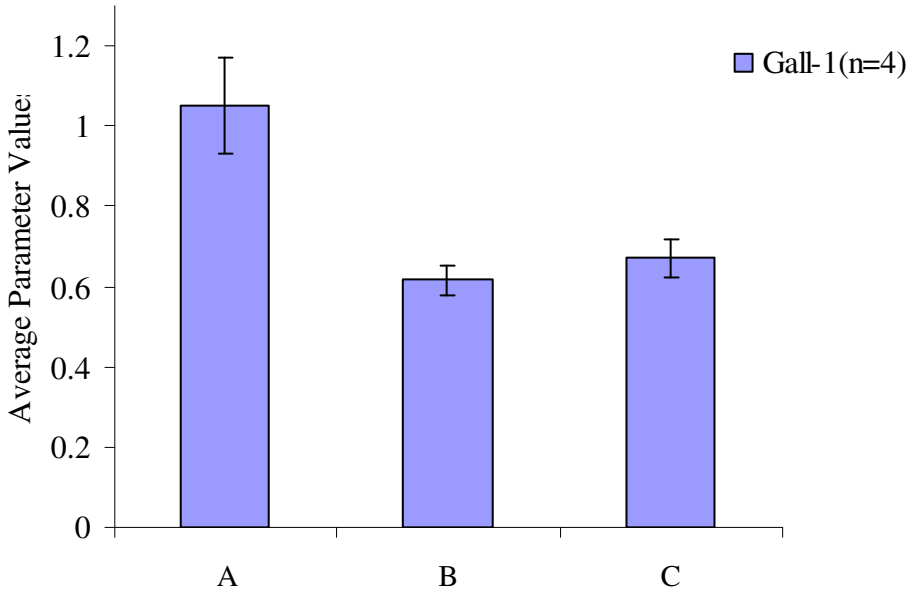

Figure 3.33 Average values of Parameters A, B and C for Gall-1 with SEM as error bars.

Table 3.26 Gall-2 data

Organ	A	B	C
Gall-3	2.40	0.68	1.02
Gall-4	3.32	0.06	0.55
Gall-6	4.02	0.17	1.12
Gall-8	5.10	0.40	2.04
MEAN	3.71	0.33	1.18
STDEV	1.14	0.27	0.62
SEM	0.57	0.14	0.31

Table 3.26 represents the statistical values of the data taken on pigs 3, 4, 6 and 8. These are classified as type –II gall spectra. Figure 3.34 plots the mean values of the four pigs with SEM as their error bars.

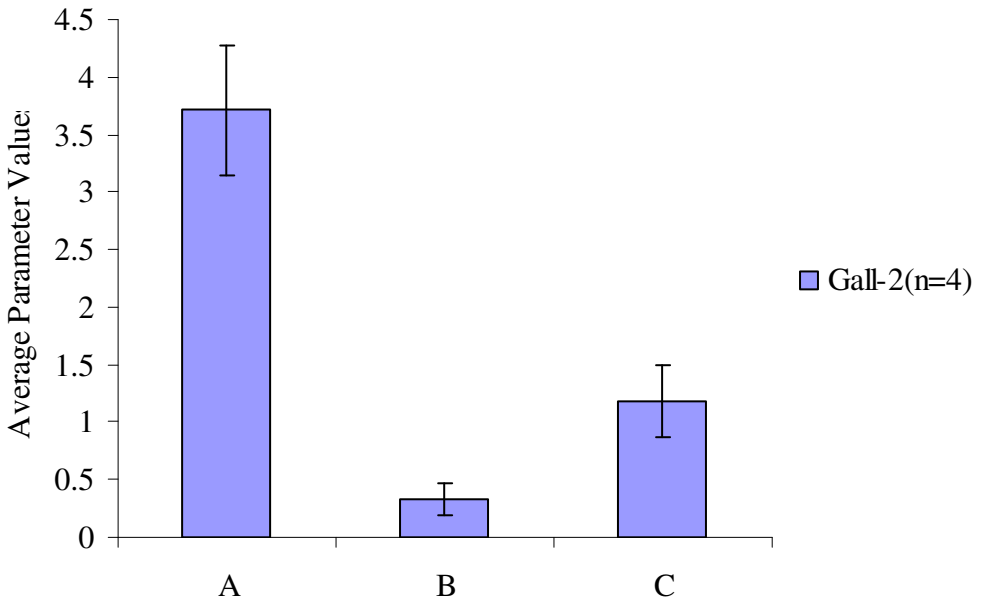

Figure 3.34 Average values of Parameters A, B and C for Gall-2 with SEM as error bars.

Table 3.27 represents the vein data measured from pigs 1, 2, 3, 6 and 7. In the case of Pig-5, the vein data was not recorded. Vein-8 is not considered as it has huge absorption until 650 nm, which is not consistent with the other pigs measurements. Figure 3.35 is a graphical representation of the mean values of the parameters A, B and C. The SEM is represented as the error bars respectively. The data are consistent over five pigs. SEM of parameter C is varying larger than the other parameters because of the shape of the spectra, as explained in 3.4.1.5.

Table 3.27 Vein data

Organ	A	B	C
Vein-1	1.12	0.43	1.23
Vein-2	1.04	0.50	1.25
Vein-3	0.78	-0.03	0.37
Vein-6	0.85	0.44	1.34
Vein-7	0.50	0.35	0.62
MEAN	0.86	0.34	0.96
S.D	0.24	0.21	0.44
SEM	0.11	0.10	0.20

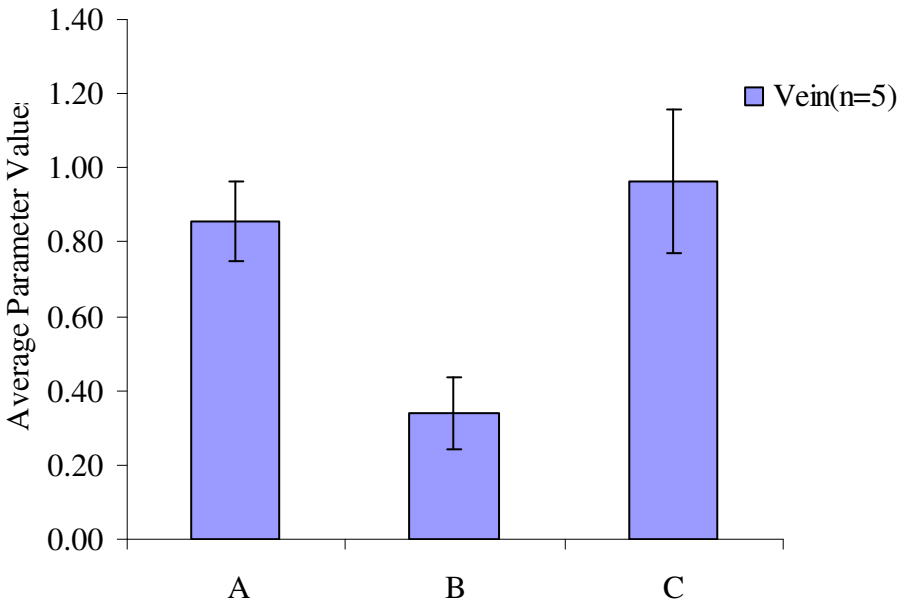

Figure 3.35 Average values of Parameters A, B and C for Vein with SEM as error bars.

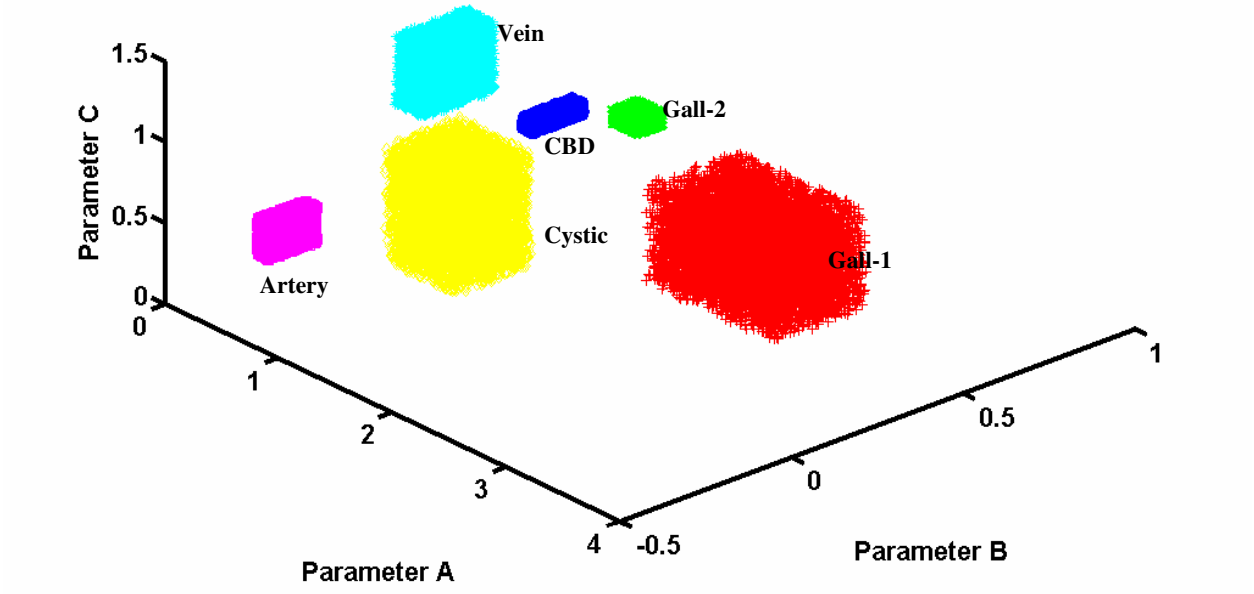

Figure 3.36: Mean of A, B and C with one standard deviation

Figure 3.36 represents the A, B and C parameters of the reflectance spectra of the biliary tract tissues and the blood vessels. The Number of Pigs (n) that were taken into consideration for Artery is 7.The eighth pig was not considered as there was a contaminated signal from the fat whose thickness was greater than what was generally found on the CBD (3-4 mm). For Gall-1, n=4. For Gall-2, n=4. For Cystic duct, n=6. The other two pigs were not considered as it was proved that the signal were contaminated from the liver because of the thin structure of the cystic duct and the large separation of the probe, which collects reflectance 5 mm beneath the tissues. For Vein, n=5. In case of vein, there were only seven pig's measurements. The other two pigs

were not considered as there was contaminated signal from the artery which runs very close by. For CBD, n=6. The other two pigs were not considered since for pig-4 and pig-6 there was an added feature of the gall. From Figure 3.36, it is quite evident that the parameters for different organs are not overlapping, which is a good demonstration for the unique spectral features.

3.4.3 Classification algorithm

Dr. Wang (Prof. in the department of Mechanical and Aerospace Engineering) has implemented the minimum distance method to classify the organs with A, B and C as the input parameters. It is shown above (section 3.4.2) that the parameters are quite consistent over some pigs, and thus the parameters can be used to classify among the organs. The results provided by Dr. Wang's algorithm are shown in Figure 3.37. In this algorithm, a random noise is mixed along with the mean values of the parameters A, B and C.

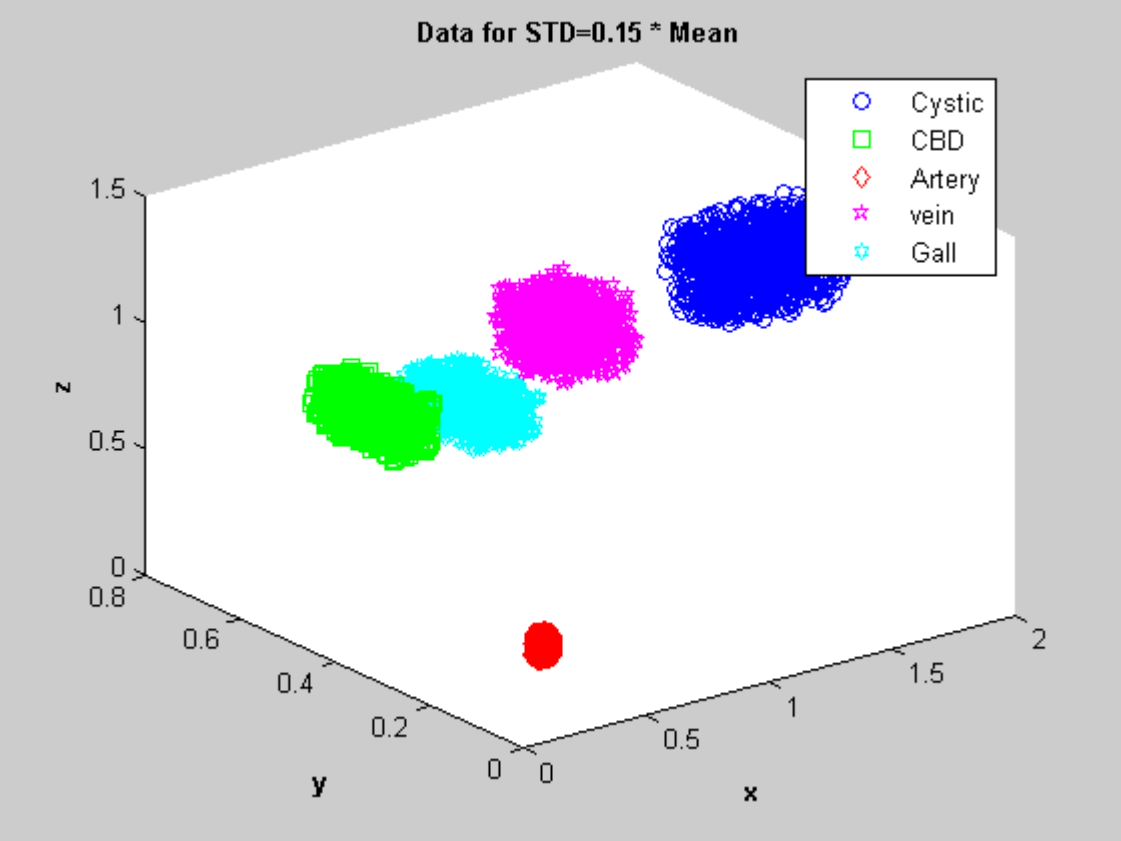

Figure 3.37 A, B and C parameters with a 15 percent deviation.

A, B and C parameters are denoted as x, y and z axis of figure 3.37, and a standard deviation of 15 percent is introduced which results in the individual clouds. The center of the cloud is the mean value of the respective organ. Two hundred points are randomly generated and is applied to the algorithm to check the procedure for classification. The classification result is shown in figure 3.38. The points are perfectly classified to their respective organs. If any circle or any data point falls out of the assigned band, that data point is unsuccessfully classified, which is not in this case with 15 percent deviation.

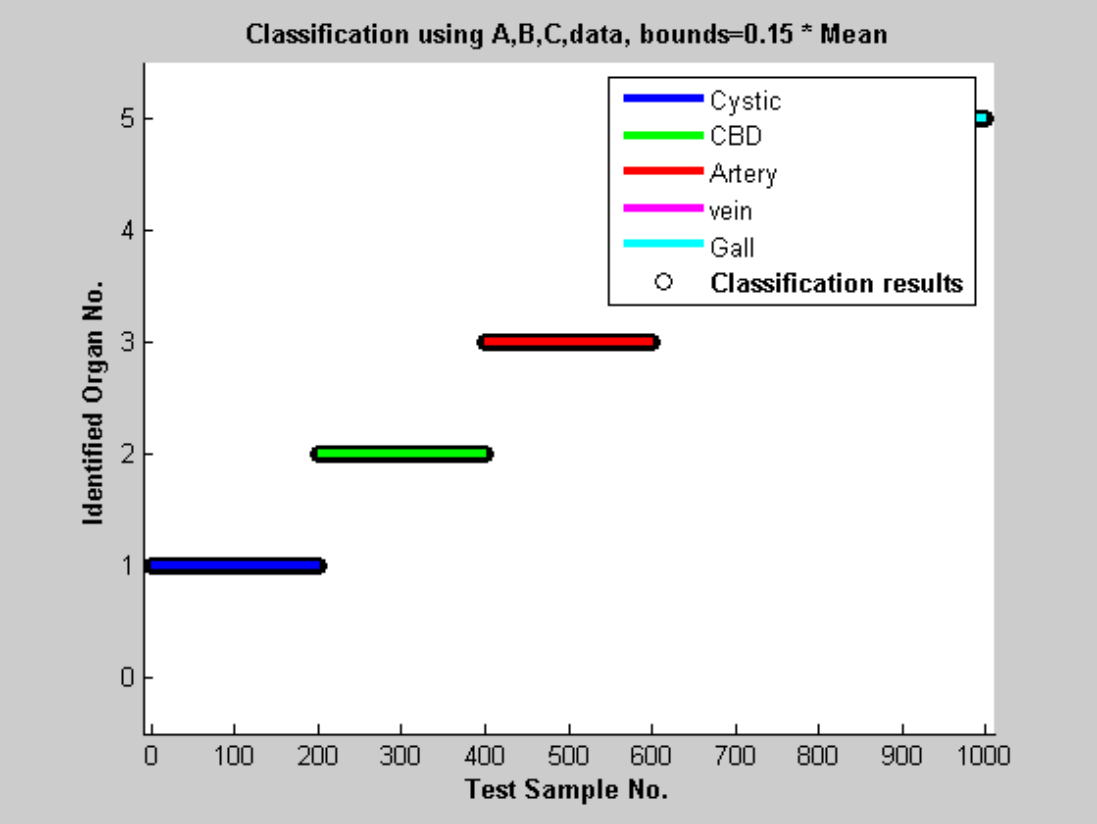

Figure 3.38 Classification using A, B and C parameters.

3.5 Special Cases

3.5.1 Contaminated signals

Some of the organs are too thin as compared to the source-detector separation that was used during the measurement. The current probe can detect five millimeters deep. A very good example for this situation is the cystic duct. Cystic duct signal is easily contaminated with the signal from the underlying liver. The reflectance data from liver and from gall could be mixed in different proportions. To prove this point, we have simulated a calculated spectrum using the mixed signals from both liver and gall.

We wish to see if it is similar to that of the cystic duct. The results are shown in figure 3.39.

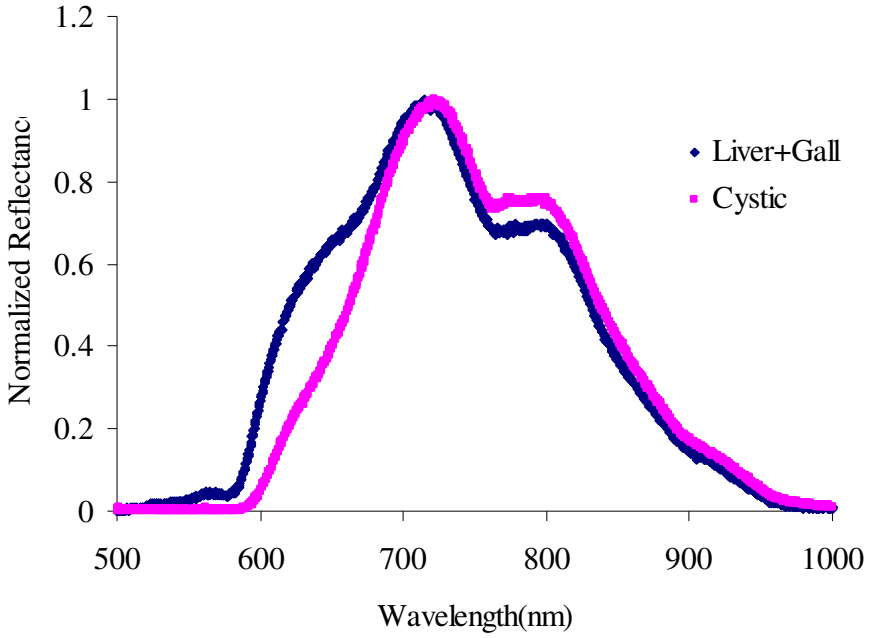

Figure 3.39 An example of contaminated signal.

In the above graph, 80 percent of the liver signal is mixed with 20 percent of the gall bladder signal, and then it is compared to that of cystic. It is observed the cystic duct measurement is in accordance with the simulated contaminated signal. This proves that the signal that we obtain from cystic could be contaminated with the signal from liver. Another example for this case is the artery spectra, which was taken on a few millimeter fat.

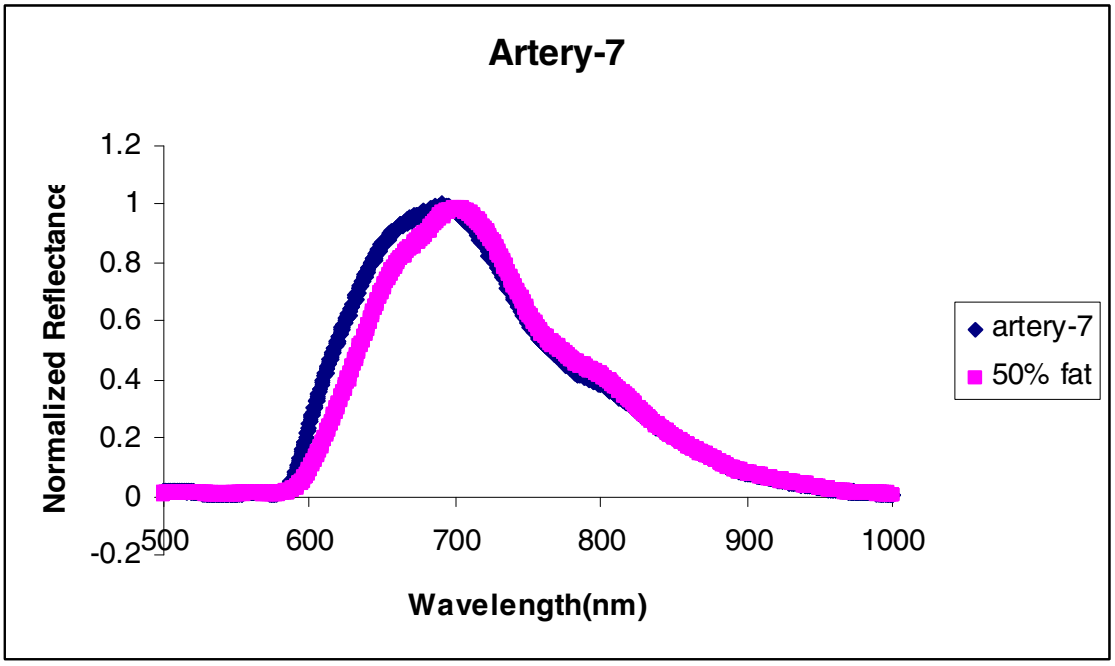

Figure 3.40 Artery signal contaminated with fat.

The artery signal from pig-7 is contaminated with fat signal and this is clearly shown in figure 3.40.

3.5.2 Gall Spectra

Gall bladder has shown two different kinds of profile for the eight pigs. The major content in the gallbladder is bile. A change in bile's chemical nature can change the reflectance signal, and not all the bile's chemical combination is the same for every pig. There is also a color difference in the gall bladder from pig to pig. This may account for the differences in the spectra of the gall bladder.

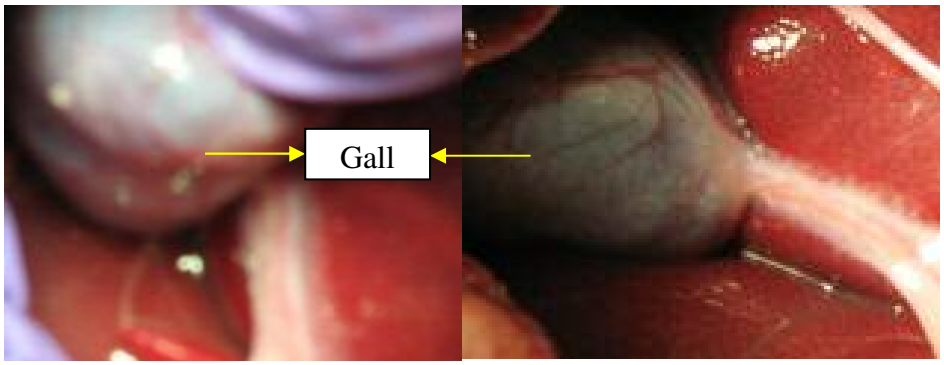

Figure 3.41 Gall Bladder Type-I (Left) and Gall Bladder Type-II (Right)

Figure 3.41 represents the color of type-I and type-II Gallbladder. They differ in colors. Type-I is lighter than Type-II. This may account for the change in their spectral profiles as shown in figure 3.42 and 3.43.

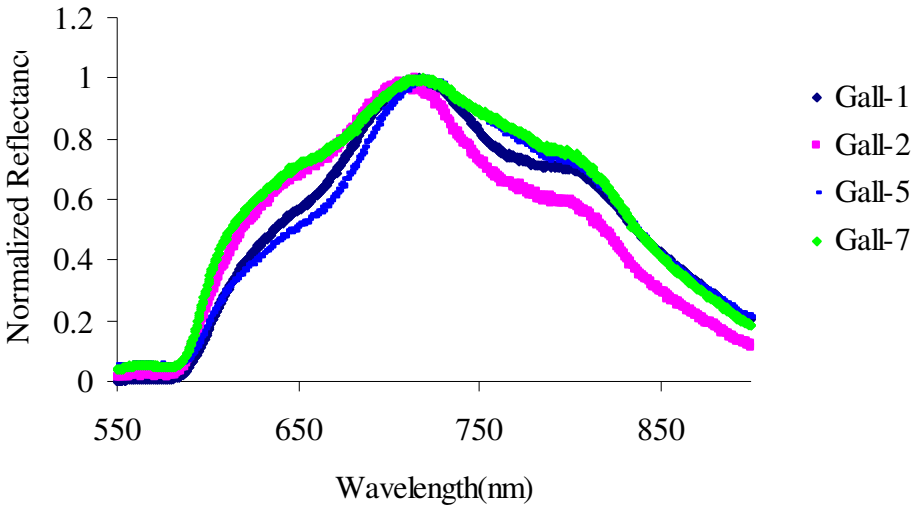

Figure 3.42 Spectra of Type-I Gall Bladder

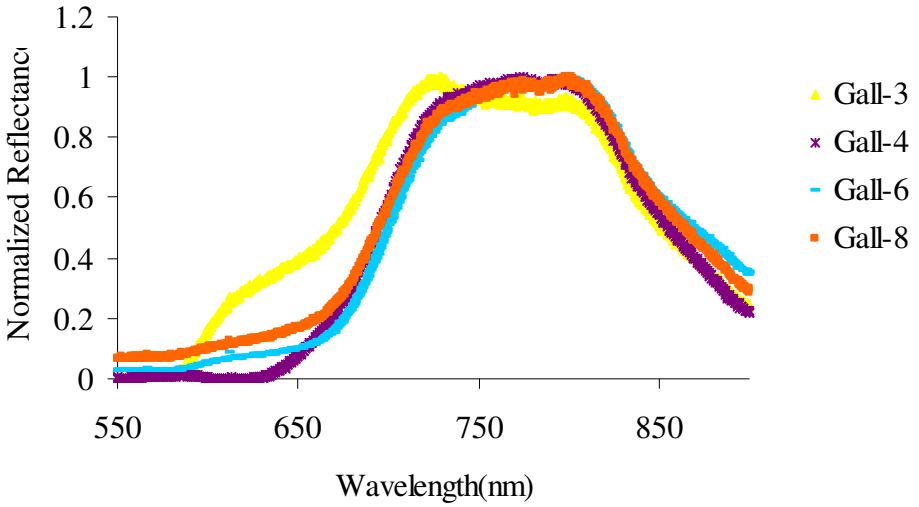

Figure 3.43 Spectra of Type-II Gall Bladder

3.5.3 Dead Pigs data

In vivo data was collected also from four dead pigs. As there was no blood circulation to the biliary tract tissues in the dead pigs, the data is not comparable to that of the in vivo live pig data.

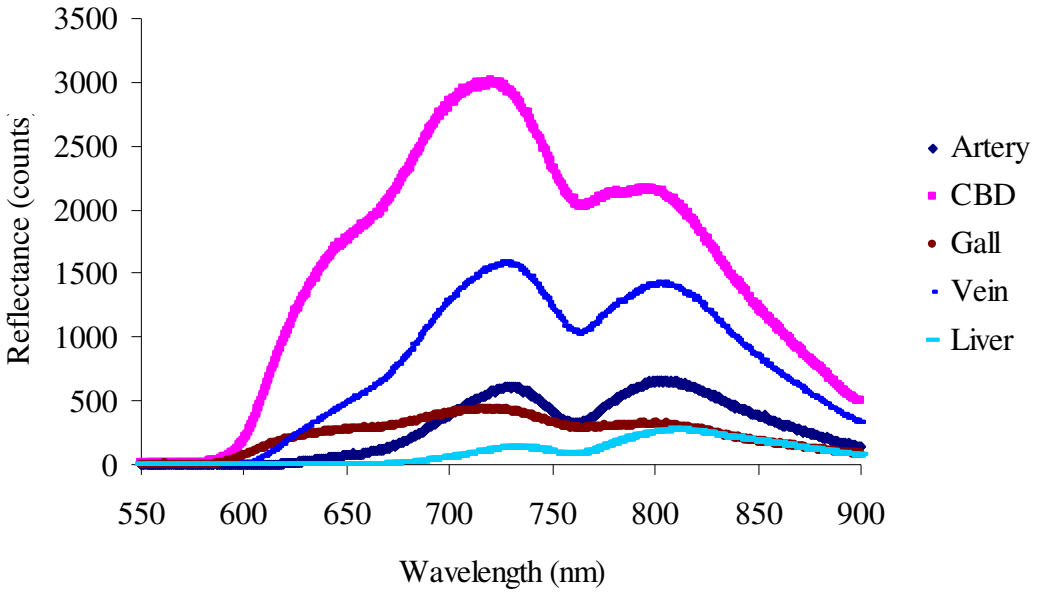

Figure 3.44 Reflectance measurement from dead pig-1.

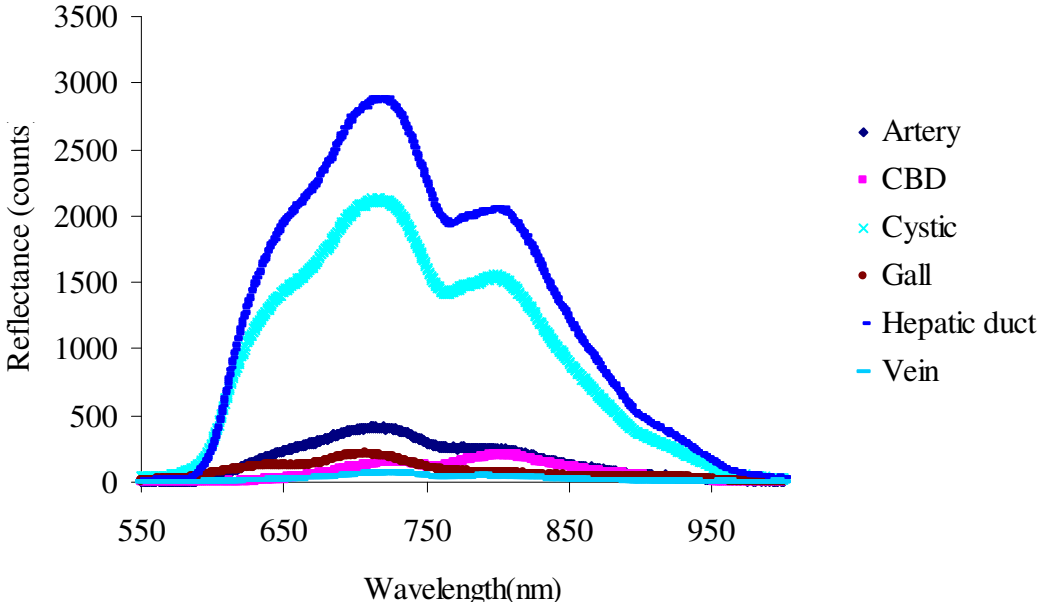

Figure 3.45 Reflectance measurement from dead pig-2.

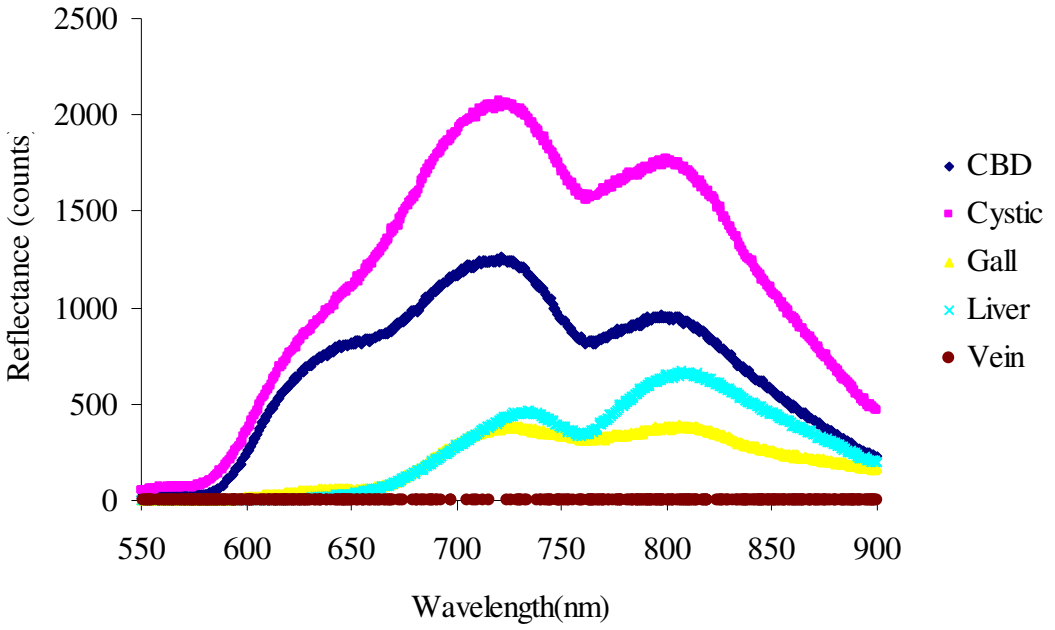

Figure 3.46 Reflectance measurement from dead pig-3.

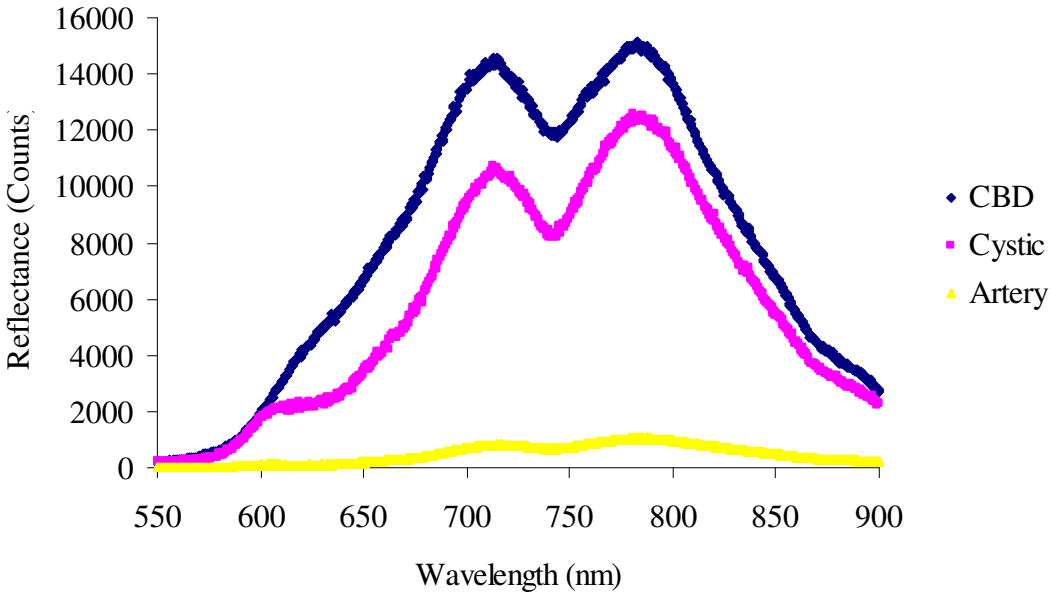

Figure 3.47 Reflectance measurement from dead pig-4.

Figures 3.44, 3.45, 3.46 and 3.47 represent the data taken on the dead pigs. It is evident from these graphs that the deoxy feature, which is a dip at around 750 nm, is quite predominant in these organs. This is not generally the case with the live pigs.

CHAPTER IV

CONCLUSION AND FUTURE WORK

From Figure 3.36, the derived components (A, B and C) obtained from the nine parameters show a promise for classification of both the biliary tract tissues and the blood vessels. These components may serve as a possible classifier to differentiate the biliary tract tissues from the blood vessels and from one another. This study demonstrates the feasibility of using Near Infrared Spectroscopy as a possible tool to differentiate between the biliary tract tissues and to be developed as a laparoscopic probe during surgery. The unique spectral features measured from the biliary tissues are consistent in multiple animals.

In summary, this study aimed to investigate the spectroscopic characterization of biliary tract tissues measured in vivo using animal models. The goal of the study was to develop an intraoperative imaging tool to be used for guiding laparoscopic cholecystectomy. Specifically, 8 live pigs were used for the in vivo experiments. The animal biliary tract tissues, including gall, common bile duct (CBD), and cystic duct, were measured using a CCD-array spectrometer and a hand-held fiber-optic probe. The respective spectroscopic features were obtained and analyzed using the Radial Basis Function. Three derived parameters were developed and can be used to differentiate different types of biliary tract tissues.

Future work may include a better design for the probe, which can be used to scan the biliary tract tissues for their unique optical signatures in real time. To find the penetration depth of the probe is an important aspect, as we need to know how deep the probe could measure. Fuzzy logic may also be implemented for classification purposes.

REFERENCES

1. Mirizzi P. “Operative cholangiography”, Surgery Gynecology & Obstetrics, 65, 702-10, 1937.

2. Flum DR, Koepsell T, Heagerty P, Sinanan M, and Dellinger EP, “Common bile duct injury during laparoscoic cholecystectomy and the use if intraoperative cholangiography: adverse outcome or preventable error?” Arch Surg. 136, 1287-92, 2001.

3. Livingston EH and Rege RV, “Costs and utilization of intraoperative cholangiography,” J of Gastrintestinal Surgery, 2-6 [In press].

4. Johns M, Giller CA, and Liu H, “Computational and in vivo investigation of optical reflectance from human brain to assist neuro surgery,” J. Biomed. Optics, 3, 437-445, 1998.

5. Giller GA, Johns M, Lih H, “Use of an intracranial near-infrared probe for localization during stereotactic surgery for movement disorders,” J.Neurosurg., 93, 498-505, 2000.

6. Tromberg B, Shah N, Lanning R, Cerussi A, Espinoza J, Pham T, Svaasand L, Butler J. “Non-invasive in vivo characterization of breast tumors using photon migration spectroscopy, ”Neoplasia, 2, 26-40, 2000.

7. Fantini S, Walker SA, Franceschini MA, Kaschke M, Schlag PM, Moesta KT, “Assessment of the size, position, and optical properties of breast tumors in vivo by noninvasive optical methods,” Appl. Opt., 37, 1982-1989, 1998.

8. McBride TO, Pogue BW, Jiang S, Österberg UL, Paulsen KD. “Initial studies of in vivo absorbing and scattering heterogeneity in near-infrared tomographic breast imaging,” Optics Letters, 26, 822-824, 2001.

9. Homma S, Fukunaga T, Kagaya A. "Influence of adipose tissue thickness on near infrared spectroscopic signals in the measurement of human muscle," J. Biomed. Opt.1(4), 418-424, 1996.

10. Gopinath S, Robertson CS, Grossman RG, Chance B. "Near-infrared spectroscopic localization of intracranial hematomas," J. Neurosurg., vol. 79, pp. 43-47, 1993.

11. Cheung C, Culver JP, Takahashi K, Greenberg JH, Yodh AG. "In vivo cerebrovascular measurement combining diffuse near-infrared absorption and correlation spectroscopies," Phys. Med. Biol. Vol. 46, 2053-2065, 2001.

12. Boas DA, Gaudette T, Strangman G, Cheng X, Marota JJA, Mandeville JB. "The accuracy of near infrared spectroscopy and imaging during focal changes in cerebral hemodynamics," NeuroImage, vol. 13, pp. 76-90, 2001.

13. Zonios G, Perelman LT, Backman V, Manoharan R, Fitzmaurice M, Van Dam J and Feld MS. "Diffuse Reflectance Spectroscopy of Human Adenomatous Colon Polyps In Vivo," Appl. Opt., 38(31), 6628-6637,1999.

14. Johns M, Giller CA, and Liu H, "Computational and in vivo investigation of optical reflectance from human brain to assist neurosurgery," J. Biomed. Optics, 3, 437-445, 1998.

15. Giller GA, Johns M, Liu H, "Use of an intracranial near-infrared probe for localization during stereotactic surgery for movement disorders," J. Neurosurg., 93, 498- 505, 2000.

16. Giller GA, Liu H, Gurnani PP, Victor S, Yazdani U, and German DC, "Validation of a Near-Infrared Probe for Detection of Thin Intracranial White Matter Structures," J. Neurosurg., 98, 1299-1306, 2003.

17. Senapati AK, Radhakrishnan H, Liu H, and Peng YB, "Detection of Degeneration in rat sciatic nerve by in vivo near infrared spectroscopy," Brain Research Protocols, 14(2), 119-125, 2005.

18. Radhakrishnan H, Peng YB, Senapati AK, Kashyap D, and Liu H, "Light scattering from rat spinal cord and sciatic nerves measured in vivo by near infrared reflectance spectroscopy," J. of Biomed. Opt., 10(5), 051405(1-8), 2005.

19. Gagnon RE and Macnab AJ, "Near Infrared Spectroscopy (NIRS) in the clinical setting - An adjunct to monitoring during diagnosis and treatment," Spectroscopy, 19 (5-6), 221-233, 2005.

20. Maitland DJ, Walsh, Jr. JT, and Prystowsky JB, "Optical properties of human gallbladder tissue and bile," Appl. Opt. 32, 586-591, 1993.

21. http://www.cs.ualberta.ca/~sutton/book/8/node7.html

22. Qian Z, Victor SS, Gu Y, Giller CA, and Liu H, " 'Look-Ahead Distance' of a fiber probe used to assist Neurosurgery: Phantom and Monte Carlo study," Optics Express, 11(16) 1844-1855, 2003.

23. Bahadur AN and Liu H, "Determination of optical probe interrogation field of near-infrared reflectance: Phantom and Monte Carlo study," Applied Optics, under review (2006).

24. Mayoraz E and Alpaydin E, "Support vector machines for multi-class classification," IWANN, 2, 833-842, 1999.

BIOGRAPHICAL INFORMATION

Sarita Kommera was born on August 1, 1981 in Hyderabad, India. She received her Bachelor of Technology degree in Electronics and Instrumentation Engineering from Jawaharlal Nehru Technological University, India in July 2003. In Spring 2004, she started her graduate studies in Biomedical Engineering from Joint Program of Biomedical Engineering at the University of Texas at Arlington and University of Texas Southwestern Medical Center at Dallas, completing it by December 2006. Her research interest includes Near Infrared Spectroscopy and medical imaging techniques.